Available online at www.sciencedirect.com
ScienceDirect
Journal of Sound and Vibration 310 (2008) 462–492
JOURNAL OF SOUND AND VIBRATION
www.elsevier.com/locate/jsvi

The canonical problem of the fluid-conveying pipe and radiation of the knowledge gained to other dynamics problems across Applied Mechanics

M.P. Païdoussis

Department of Mechanical Engineering, McGill University, 817 Sherbrooke Street W., Montreal, QC, Canada H3A 2K6

Accepted 12 March 2007
The peer review of this article was organised by the Guest Editor
Available online 15 June 2007

Abstract

The basic dynamics of pipes conveying fluid is reviewed, establishing why this system has become a *model dynamical problem*. The paper then discusses the radiation of the experience gained in studying this problem into other areas of Applied Mechanics, particularly other problems in fluid–structure interactions involving slender structures and axial flows; specifically the dynamics of (i) quasi-cylindrical bodies in axial flow or towed in quiescent fluid; (ii) cylindrical shells containing or immersed in axial flow; and (iii) plates in axial flow. Applications, some of them wholly unexpected when the work was done, are noted throughout.

1. Introduction

What is the underlying reason for all the interest in the dynamics of pipes conveying fluid? Why are there approximately 550 significant publications on the subject (counting up to 2003)? The reason, as noted by Païdoussis and Li [1], is that this has become a "model dynamical problem", *a new paradigm in dynamics*. In its simplest form, the governing equation of motion is simple enough to solve, yet can demonstrate generic features of much more complex dynamical systems; moreover, the theoretical results can in many cases be validated by relatively easy-to-mount and to-perform experiments. As a result, this problem has been used as a tool for understanding the behaviour of more complex systems, or as a vehicle in the search of new phenomena and new dynamical features. A concrete example of this is the combined theoretical and experimental study undertaken by Bishop and Fawzy [2], the ultimate purpose of which was the development of methods for the prediction of aircraft flutter characteristics based on pre-flutter flight data—thus avoiding dangerous full-scale or wind-tunnel experimentation in the critical zone.

The focus of this paper, however, will be on less remotely connected problems than aircraft flutter; rather, it will concentrate on the dissemination of the understanding, methodology and experience gained in studying the dynamics of fluid-conveying pipes to a set of related systems, namely *slender structures subjected to axial*

E-mail address: mary.fiorilli@mcgill.ca.

0022-460X/$ - see front matter © 2007 Elsevier Ltd. All rights reserved.
doi:10.1016/j.jsv.2007.03.065

flow or *travelling slender structures in quiescent fluid*. In many cases, this lateral transfer of experience has also served to bring to light similarities and significant differences in the classes of systems concerned.

The structure of this paper is as follows. First, the dynamics of pipes conveying fluid is reviewed in Section 2. This is followed by the discussion of the dynamics of kindred systems in Sections 3–5, pointing out significant similarities and differences, as well as recounting the ever widening circle of applications to engineering and physiological systems.

2. Dynamics of pipes conveying fluid

This is a highly abbreviated account of the dynamics of fluid-conveying pipes, adapted to the purposes of this paper. For a fuller account, the reader is referred to Refs. [3;4, Appendix Ω].

2.1. Basic dynamics and energy considerations

Consider a pipe, modelled as an Euler–Bernoulli beam, conveying fluid. The pipe may be either supported at both ends or cantilevered.

If gravity, internal damping, a possible elastic foundation, externally imposed tension and pressurization effects are either absent or neglected, the linear equation of motion of the pipe takes the particularly simple form [5,6]

$$EI\frac{\partial^4 w}{\partial x^4} + MU^2\frac{\partial^2 w}{\partial x^2} + 2MU\frac{\partial^2 w}{\partial x \partial t} + (M+m)\frac{\partial^2 w}{\partial t^2} = 0, \tag{1}$$

where EI is the flexural rigidity of the pipe, M is the mass of fluid per unit length, flowing with a steady flow velocity U, m is the mass of the pipe per unit length, and w is the lateral deflection of the pipe; x and t are the axial coordinate and time, respectively. The fluid forces are modelled in terms of a plug flow model, which is the simplest possible form of the slender body approximation for the problem at hand. A fuller form of the linear equation of motion is given in Appendix A.

Sequentially, the terms in Eq. (1) are associated with: flexural restoring forces, flow-related centrifugal forces (associated with pipe curvature), flow-related Coriolis forces, and inertial forces. What is often forgotten is that in the derivation of this equation the fluid has *not* been assumed to be inviscid; however, viscous traction on the pipe and viscous pressure-loss forces exactly cancel out in the linear limit, as first pointed out by Benjamin [5,7], and hence do not explicitly appear in Eq. (1).

Presuming the existence of periodic motions, the rate of work done by the fluid on the pipe over a period of oscillation T may be obtained from Eq. (1):

$$\Delta W = -MU\int_0^T \left[\left(\frac{\partial w}{\partial t}\right)^2 + U\left(\frac{\partial w}{\partial t}\right)\left(\frac{\partial w}{\partial x}\right)\right]\Bigg|_0^L \mathrm{d}t. \tag{2}$$

Clearly if the ends of the pipe are positively supported, then $(\partial w/\partial t) = 0$ at both ends, and

$$\Delta W = 0. \tag{3}$$

This implies that self-excited oscillatory motion (flutter) is not possible for pipes with both ends supported. This fact does not imply that the system remains stable, no matter how high U may become. Indeed, looking at Eq. (1) it is remarked that, if an externally applied tension were present, there would be an additional term $-\overline{T}(\partial^2 w/\partial x^2)$ in the equation; thus, clearly, the $+MU^2(\partial^2 w/\partial x^2)$ term is an *effective compression*, associated with the exiting fluid momentum at the downstream end. Then, by analogy to a column subjected to a compressive load, we can see that for high enough U the system would lose stability by static divergence (buckling).

A pipe with supported ends is a *gyroscopic conservative* system in Ziegler's classical classification of dynamical systems [8]. The conservativeness of the system is demonstrated by Eq. (3). All fluid-dynamic forces do no work, including the Coriolis forces which are responsible for the gyroscopicity of the system. Nevertheless, these forces are responsible for the non-existence of classical modes, i.e. modes with stationary

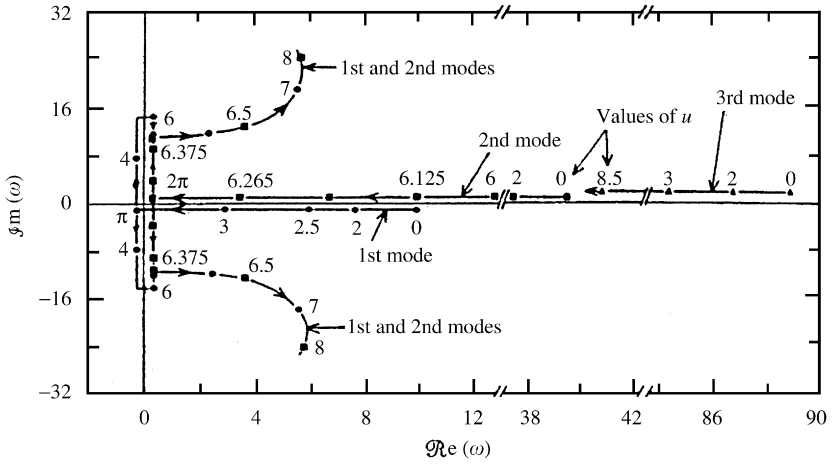

Fig. 1. Dimensionless complex frequency diagrams for a pinned–pinned pipe; $\beta = 0.1$ and $\Gamma = \Pi = \alpha = \sigma = k = \gamma = 0$ [see Eqs. (A.3) for meaning of symbols] as a function of the dimensionless flow velocity u. The loci that actually lie on the axes have been drawn slightly off the axes but parallel to them for the sake of clarity. —●—, first mode; —■—, second mode; —▲—, third mode; — ■—●— ■—, combined first and second modes; from Ref. [12].

nodes; rather, the mode shapes involve travelling wave components (see, e.g., Ref. [3, Fig. 3.13]). Another characteristic of such systems is that, if they lose stability, they must do so by static divergence.[1]

On the other hand, for a cantilevered system, assuming the free end is at $x = L$, one obtains

$$\Delta W = -MU \int_0^T \left[\left(\frac{\partial w}{\partial t} \right)_L^2 + U \left(\frac{\partial w}{\partial t} \right)_L \left(\frac{\partial w}{\partial x} \right)_L \right] \mathrm{d}t \neq 0, \tag{4}$$

where $(\partial w/\partial t)_L$ and $(\partial w/\partial x)_L$ are, respectively, the lateral velocity and slope of the free end. In Ziegler's [8] classification, since some of the forces associated with $\Delta W \neq 0$ are not velocity-dependent [the $MU^2(\partial^2 w/\partial x^2)$ follower load leading to the second term in Eq. (4)], this is a non-conservative *circulatory* system. The dynamics of this system was elucidated by means of this expression by Benjamin [5] and elaborated by Païdoussis [9].

For $U > 0$ and sufficiently small for the second term within the square brackets to be much smaller than the first, it is clear that $\Delta W < 0$, and free motions of the pipe are damped—an effect due to the Coriolis forces, which, unlike the case of supported ends, in this case *do* do work. If, however, U is sufficiently large, while over most of the cycle $(\partial w/\partial x)_L$ and $(\partial w/\partial t)_L$ have opposite signs, then $\Delta W > 0$; i.e. the pipe will gain energy from the flow, and free motions will be amplified. The requirement that $\overline{(\partial w/\partial x)_L (\partial w/\partial t)_L} < 0$ suggests that, in the course of flutter, the pipe must execute a sort of 'dragging', lagging motion that one would obtain when laterally oscillating a flexible blade or baton in dense fluid. This, indeed, is what is observed, as remarked by Bourrières [10], Benjamin [7] and Gregory and Païdoussis [11].

2.2. Pipes with supported ends

The dynamics of the system for a pipe simply supported at both ends is illustrated in the Argand diagram of Fig. 1, for solutions of the form $\eta(\xi, \tau) = Y(\xi) \exp(\mathrm{i}\omega\tau)$, where $\eta = w/L$, $\xi = x/L$, τ is the dimensionless time, and ω is the dimensionless eigenfrequency, which is generally complex; this being an infinite-dimensional problem, there is an infinity of ω_i, $i = 1, 2, \ldots \infty$, which are found by solving Eq. (1) subject to appropriate boundary conditions.

In Fig. 1, u is the dimensionless flow velocity, $u = (M/EI)^{1/2} UL$; refer to Appendix A for the definition of all dimensionless quantities. It is recalled that Re(ω) is the dimensionless oscillation frequency, while Im(ω) is

[1]This, however, is not absolutely always true; refer to Ref. [13].

related to damping, the damping ratio being $\zeta = \mathrm{Im}(\omega)/\mathrm{Re}(\omega)$. The main dynamical features displayed in Fig. 1 are: (i) since dissipation is absent in this example, the eigenfrequencies are purely real and they are diminished with increasing u, for $0 \leqslant u < \pi$; (ii) at $u = u_{cd} = \pi$ the system loses stability in its first mode by divergence, via a pitchfork bifurcation, and thereafter the eigenfrequencies become purely imaginary.

For higher flow velocities, there is a second divergence, associated with the second mode, at $u = 2\pi$. At slightly higher u, the first and second-mode loci coalesce and the lower branch is associated with $\mathrm{Re}(\omega) \neq 0$ and $\mathrm{Im}(\omega) < 0$, implying coupled-mode flutter for $u > 6.375$. This form of coupled-mode flutter has been called "Païdoussis flutter" by Done and Simpson [14] to differentiate it from the "Hamiltonian Hopf" type, and the name stuck.

This is one of the many paradoxes associated with this system: whereas Eq. (3) shows that flutter is not possible, linear analysis shows that it is. This is paradoxical, even though, strictly speaking, one cannot rely on the predictions of linear theory beyond the onset of the first instability, i.e. for $u > \pi$. An attempt to resolve this paradox was made by Done and Simpson [14], but it was Holmes who gave the definitive answer with the aid of a simplified nonlinear form of the equation of motion, taking into account only the tension induced by lateral deformation of the pipe. By means of a finite-dimensional analysis [15] and then an infinite-dimensional analysis [16] utilizing the Lyapunov second (direct) method, Holmes showed that "Pipes supported at both ends cannot flutter", which is also the title of one of his two papers on the subject; see Ref. [3, Chapter 5].

There remained a slight question mark on the non-occurrence of flutter, because Holmes utilized a simplified equation of motion. This doubt, however, was laid to rest by the work of Yoshizawa et al. [17] and Modarres-Sadeghi et al. [18]. In the former, no coupled-mode flutter was found up to $u \simeq 1.3u_{cd}$, where u_{cd} is the critical flow velocity for divergence, in a clamped–pinned pipe. In the latter, this was proved even more definitively by carrying out calculations up to $u \simeq 3u_{cd}$ for a pinned–pinned pipe (i.e. a pipe with both ends simply supported), utilizing the full nonlinear equations of motion (Eqs. (A.5) and (A.6)).

All the work cited in the last two paragraphs relates to theoretical work. However, perhaps the most potent evidence of non-occurrence of post-divergence of flutter in pipes with both ends supported is that it has never been observed experimentally, though the loss of stability by divergence is easily observable.

2.3. Cantilevered pipes

The dynamics in this case is illustrated by another Argand diagram, Fig. 2. Here it is seen that the effect of increasing u, provided it remains small, is to generate flow-induced damping in the system (in this case it was assumed that there was none at $u = 0$), since $\mathrm{Im}(\omega) > 0$ and increasing with u. For $u \simeq 4$, however, this

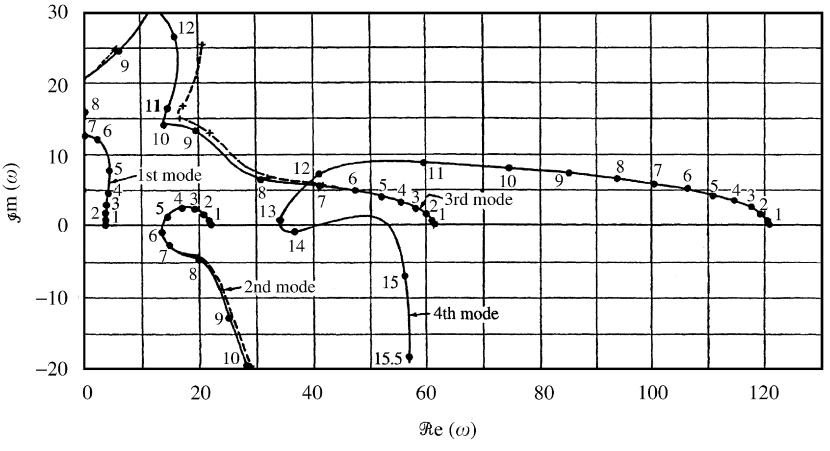

Fig. 2. The dimensionless complex frequency of the four lowest modes of the cantilevered system ($\gamma = \alpha = \sigma = k = 0$) as a function of the dimensionless flow velocity, u, for $\beta = 0.2$: —, exact analysis; - - -, four-mode Galerkin approximation; from Ref. [6].

damping begins to be attenuated; it eventually vanishes (at $u \simeq 5.6$) and then becomes negative, indicating the onset of single-degree-of-freedom flutter via a Hopf bifurcation. The presence of a non-zero damping at $u = 0$, merely postpones the onset of flutter.

In this case, there is no contradiction between the results of Fig. 2 and the dynamical behaviour suggested by Eq. (4).

The nonlinear dynamics of the system is, to this extent, concordant: the Hopf bifurcation gives rise to limit-cycle oscillations, which is also what is observed experimentally. However, the dynamics can be much more complex in this case (see, e.g., Ref. [3, Chapter 5]). The Hopf bifurcation can be either subcritical (implying a softening nonlinear behaviour and hysteresis as u is decreased) or supercritical, depending on the parameter $\beta(= M/(M+m))$ and a parameter involving the friction coefficient and the slenderness of the pipe [19]. Also, the limit cycle can be either two- or three dimensional [20], again depending on β. In the latter case, motions are circular for a perfectly uniform system, or more complex for imperfect systems [20,3].

2.4. Some physical characteristics of the dynamics

It is important to describe the dynamical behaviour of the system in physical terms, as one would observe it experimentally.

For a system with supported ends, as the flow velocity is increased the eigenfrequencies become smaller. As a result, although the damping is not affected, the logarithmic decrement increases. Any imperfections in the pipe become more noticeable since the effective restoring force (towards the stretched-straight equilibrium configuration) becomes weaker—eventually nearly vanishing at the critical point for the onset of divergence. In reality, the system never loses stiffness entirely, and the transition from stability to instability is, at best, manifested by a sharp increase in the imperfection-related lateral deformation of the pipe; the less imperfect the system, the sharper the transition, and the easier it is to identify the threshold of divergence. By the same token, the first-mode eigenfrequency never quite vanishes; it reaches a minimum and, once the threshold is crossed, it may actually increase—the post-divergence behaviour depending on the nature of the end-supports, e.g. on whether axial sliding is permitted or prevented. The amplitude of buckling increases with flow.

The principal physical feature displayed by this system is flow-induced *negative stiffness*, increasing with flow and eventually overwhelming the flexural restoring force. A remarkable demonstration of this behaviour is provided by Thompson's black box [21], as illustrated in Fig. 3: adding more weight, the scale moves *up*; within the box is a fluid-conveying articulated pipe, equivalent to a continuously flexible one, the bottom end of which is attached to the scale. Another demonstration is by touching with a finger the bottom of a hanging cantilevered pipe conveying fluid, at flows close to but smaller than the critical flow for divergence [3]. The pipe buckles, and it follows the finger as one tries to gently remove it, clearly demonstrating a negative stiffness.

For the cantilevered system, it is easy to observe that the system becomes more damped as the flow velocity is increased, by its response to small external perturbations (e.g. a small push); eventually, the system becomes overdamped. At higher flows, however, this process is reversed and, at the critical point, self-excited flutter

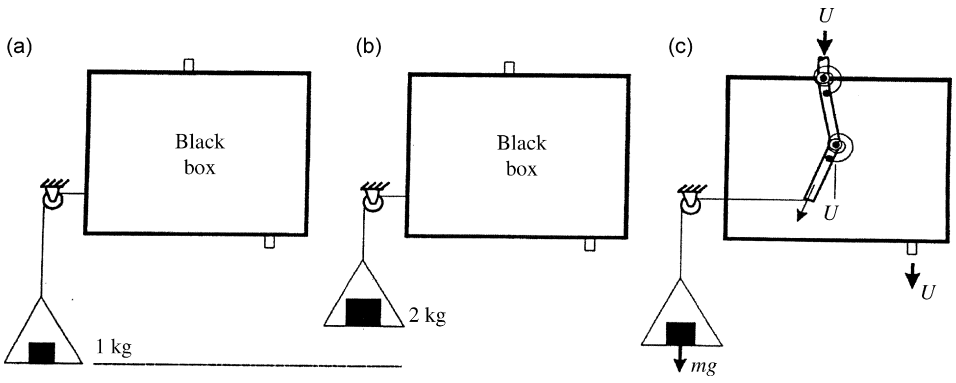

Fig. 3. Illustration of the negative stiffness mechanism of a buckled pipe conveying fluid, analysed by Thompson [21,3].

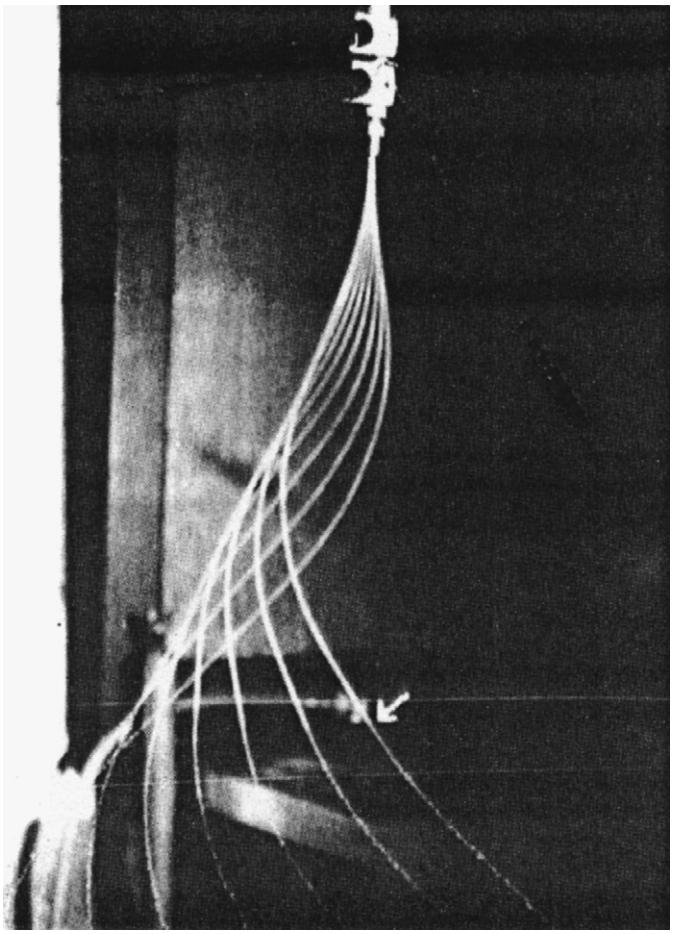

Fig. 4. Photograph of a fluttering vertical pipe from the experiments by Greenwald and Dugundji [22]. The arrow shows the end of the pipe; what is seen below that point is the free water jet.

occurs leading to a stable limit cycle. In cases corresponding to a subcritical Hopf bifurcation, one can observe the existence of an unstable limit cycle nesting within a stable outer one. The limit-cycle motion can be planar (2-D), circular, or more generally oval-shaped (3-D). The amplitude increases with flow velocity. The modal shape always shows a travelling wave component with no fixed nodes (see Fig. 4).

The principal physical characteristics in this case are (i) flow-induced *negative damping*, and (ii) Coriolis-related non-classical modal shapes (no fixed nodes). Another noteworthy characteristic of this system is the possible destabilizing effect of damping and negative energy modes—both of which are non-intuitive—demonstrating the existence of Class A instabilities in Benjamin's classification [23] (see Ref. [3, Sections 3.5.3–3.5.5 and Appendix C]).

2.5. *Addenda and modifications to the system and enriched dynamics*

The dynamics of the basic, "bare" system of a pipe conveying fluid can become more interesting and complex, particularly in the case of the non-conservative cantilevered system, by the addition of (i) elastic foundations of different types, (ii) a solid support somewhere along the length of the pipe, (iii) spring supports and/or dashpots at some point along the pipe, (iv) a point-mass or masses somewhere along the pipe, (v) a plate affixed to the pipe, (vi) motion-limiting constraints.

In the case of cantilevered pipes, the dynamics is often unexpected; i.e., additional spring supports or masses can make the system more unstable—i.e. result in smaller critical flow velocities than for the bare system.

The case of added spring supports has received considerable attention, because the nonlinear dynamics can be extremely interesting, e.g. the dynamics in the vicinity of a double degeneracy, where a Hopf and a pitchfork bifurcation occur at almost the same flow velocity, leading to complex dynamics and chaos; see, e.g., Ref. [24]. Also, the case of added masses, especially when attached to the free end of the cantilever, result in secondary bifurcations, complex motions and chaos; see, e.g., the work of Copeland and Moon [25] and Païdoussis and Semler [26].

Also, if the fluid direction is reversed (i.e. the cantilevered pipe becomes "aspirating"), interesting dynamics may arise—briefly touched upon in Appendix B. Moreover, parametric resonances may occur if the flow in the pipe is not wholly steady but contains periodic pulsations. Finally, additional features come to light when the pipe is not straight, i.e. when it is curved, or more so if it has some 3-D shape.

All these aspects, though fascinating in themselves, are beyond the scope of this paper. The interested reader will find them discussed in Ref. [3].

2.6. Applications

The instabilities discussed in the foregoing occur in the range $u = 3$–10 generally. However, the corresponding *dimensional* flow velocities are too high to be of real concern for most engineering applications, unless the pipe is long and hence flexible or in special systems.

Applications of this work are related to the static stability of deep water risers and ocean mining systems [3, Section 4.7]. Of special interest is the latter, where considerable work has been done more recently; see Appendix B.

Another direct application of this work is the Coriolis mass-flow meter, an instrument in which the Coriolis effect is used to measure the flow through a generally U-shaped pipe segment made to vibrate torsionally (although other geometries are used as well).

Yet another application is the invention of hydroelastic ichthyoid propulsion, where a cantilevered plate is attached to a pipe conveying fluid at high enough flow for the composite plate-pipe to flutter. Because of the travelling wave component in the flutter, this can be used to generate enhanced propulsion for surface or underwater craft [27].

It should be stressed, however, that, as in many areas of fundamental Applied Mechanics, applications emerge 10, 20 or 50 years after the work was done, often in areas totally unforeseen by those who conducted the original research [28]. One such potential application on which this writer and his colleagues are currently working is based on research originally done on the dynamics of flow-powered drill-strings, which may find application in MEMS/nanotechnology.

The main "application" and usefulness of this work is nevertheless in the dissemination of the experience gained to other areas of Applied Mechanics, which is the subject of the sections that follow.

3. Dynamics of slender cylinders in axial flow

3.1. Solitary cylinders

Consider a cylinder in axial flow, as in Fig. 5. If gravity and confinement (by the external channel) effects are neglected and the downstream is free, the simplest form of the linear equation of motion is [29]

$$\begin{aligned} EI\frac{\partial^4 y}{\partial x^4} + MU^2\frac{\partial^2 y}{\partial x^2} + 2MU\frac{\partial^2 y}{\partial x \partial t} + (M+m)\frac{\partial^2 y}{\partial t^2} \\ - \left[\frac{1}{2}\rho D U^2 C_T(L-x) + \frac{1}{2}\rho D^2 U^2 C_b\right]\frac{\partial^2 y}{\partial x^2} \\ + \frac{1}{2}\rho D U C_N\left(\frac{\partial y}{\partial t} + U\frac{\partial y}{\partial x}\right) + \frac{1}{2}\rho D C_D\frac{\partial y}{\partial t} = 0, \end{aligned} \tag{5}$$

where $M = \rho A$ is the virtual, or added, mass of the fluid per unit length for unconfined flow, A being the cross-sectional area of the cylinder and ρ the fluid density, $y(x,t)$ is the lateral deflection, C_T and C_N are the viscous

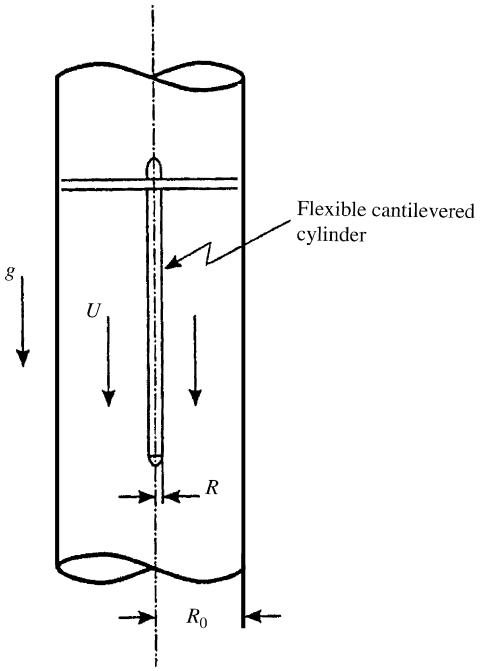

Fig. 5. Diagrammatic view of a hanging cantilevered cylinder in axial flow, in the test-section of a circulating system.

force coefficients in the longitudinal and normal direction, respectively, C_D is the linearized zero-flow viscous drag coefficient for lateral motions, C_b is the base drag coefficient, D is the cylinder diameter, and the other symbols are the same as for internal flow. If both ends are supported, the equation of motion is slightly more complicated, depending also on whether the downstream end is free to slide axially, pressurization of the external fluid, and so on; see Appendix C.

If the two ends are supported, then the standard form of the beam boundary conditions apply, as was the case for the pipe conveying fluid. If the cylinder is cantilevered, however, it is generally supposed that the free end is ogive-shaped (e.g., it is in the form of a half-ellipsoid). In that case, the simplest form of the boundary conditions are

$$EI\frac{\partial^2 y}{\partial x^2}=0, \quad EI\frac{\partial^3 y}{\partial x^3}+fMU\left(\frac{\partial y}{\partial t}+U\frac{\partial y}{\partial x}\right)-(m+fM)x_e\frac{\partial^2 y}{\partial t^2}=0, \tag{6}$$

in which $x_e=(1/A)\int_{L-l}^{L}A(x)\,\mathrm{d}x$, l being the length of the shaped end; f is a parameter first introduced by Hawthorne [30], equal to unity for a truly streamlined end, but generally smaller because of 3-D flow over the end and boundary-layer effects.

Examining Eq. (5), it is immediately obvious that its first line is identical to Eq. (1). In fact the two equations differ only because of the viscous terms constituting the rest of Eq. (5); unlike the case of internal flow, these effects are not counterbalanced by pressure loss terms, as the mean pressure in the flow is insensitive to boundary-layer development on the cylinder itself. However, generally, these terms are small compared to the first four terms in Eq. (5), and so the dynamics, for cylinders with supported ends at least, may be expected to be similar to that of the fluid-conveying pipe.[2] For cantilevered pipes, however, one of the boundary conditions is also different, so greater differences may be expected in this case.

These expectations are borne out by the typical Argand diagram of Fig. 6 for a cylinder with simply supported ends. It is seen that, because of the viscous forces (even though internal dissipation in the cylinder has been neglected), in this case $\mathrm{Im}(\omega)\neq 0$ for $u\geqslant 0$. However, divergence is predicted at a flow velocity only slightly higher than $u=\pi$ in the first mode, followed at $u\simeq 2\pi$ by divergence in the second mode.

[2]Provided the cylinder is not very long; refer to the last two paragraphs of Section 3.1.

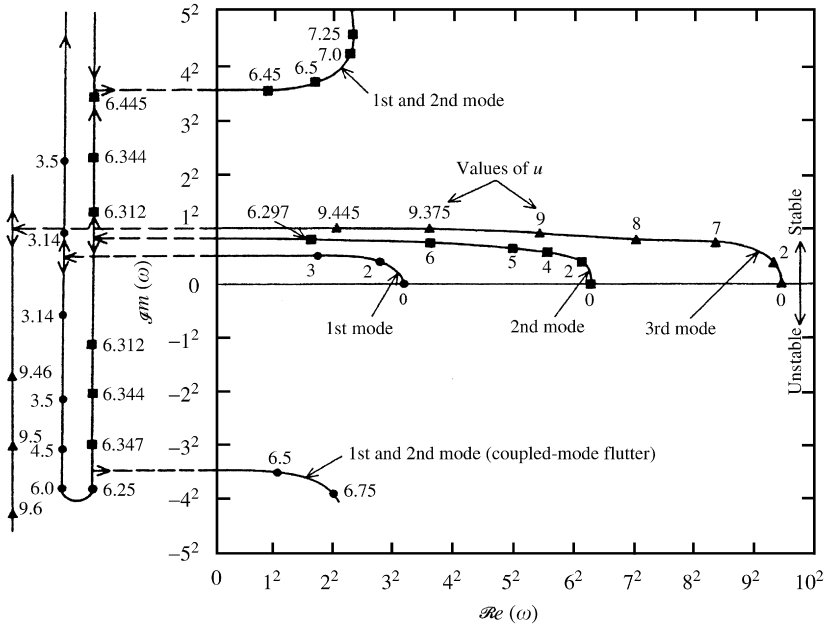

Fig. 6. Argand diagram for the complex frequencies, ω, of the lowest three modes of a solitary pinned–pinned cylinder in unconfined axial flow, as functions of u, for $\beta = 0.1, \varepsilon c_f = 1, \delta = \chi = 1, c = \alpha = h = \gamma = \Pi = \Gamma = 0$; the dimensionless parameters are defined in Eqs. (C.3). From Ref. [29].

Coupled-mode flutter is predicted at $u \simeq 6.48$. The question of its existence comes up again. In this case, however, $\Delta W \neq 0$. In fact,

$$\Delta W = -\frac{1}{2} c_N (MU/D) \int_0^T \int_0^L (\dot{y}^2 + U\dot{y}y')\,\mathrm{d}x\,\mathrm{d}t - \frac{1}{2}(M/D) \int_0^T \int_0^L (c^*\dot{y}^2 - c_T U^2 \dot{y}y')\,\mathrm{d}x\,\mathrm{d}t, \tag{7}$$

where $c_N = (4/\pi)C_N, c_T = (4/\pi)C_T$ and $c^* = (4/\pi)C_D$; the overdot stands for $\partial(\ )/\partial t$ and the prime for $\partial(\ )/\partial x$. Clearly, the predicted dynamical behaviour is quite similar to that for internal flow (cf. Fig. 1). Thus, in this case the coupled-mode flutter predicted in Fig. 6 is not contradicted by energy-transfer considerations: by virtue of Eq. (7), coupled-mode flutter is quite plausible. Indeed, post-divergence flutter has been observed in experiments [31]; see Fig. 9(a). Moreover, significantly, ΔW in Eq. (7) is wholly related to viscous effects, which do not play a role in the dynamics of systems with internal flow (Section 2).

Recent calculations by means of nonlinear theory have confirmed the existence of post-divergence flutter [32], and more recently still reconfirmed its occurrence experimentally [33]. The bifurcation diagram shown in Fig. 7(a) clearly shows that a Hopf bifurcation arises from the post-divergence static solution branch, contrary to linear analysis which predicted that it arises from loss of stability of the trivial equilibrium state. The Hopf bifurcation at $\mathscr{U} = 14.2$[3] is supercritical. At higher flows, the system displays quasiperiodic and chaotic oscillations (Fig. 7(c,d)), followed by a range of $\mathscr{U}$ where the statically deformed shape is regained.

The dynamics of a typical cantilevered system is illustrated in Fig. 8. It is seen that the system first loses stability by divergence at $u \simeq 2.04$, and then by single-mode flutter (via a Hopf bifurcation) at $u \simeq 5.16$, and after restabilization by flutter in the third mode at $u \simeq 8.17$. It can be shown that the divergence is related to the presence of the tapered free end (in this case $f = 0.8$ suggests a fairly well streamlined end); the underlying mechanism is related to the lift of low-aspect ratio wings [34,4]. If the end is blunt ($f = 0$), then divergence is not possible.

[3]In the *nonlinear* theory for cylinders with both ends supported, both the lateral (v) and the longitudinal (u) deformations have to be taken into account; hence, to avoid confusion, the dimensionless flow velocity defined by u in Eq. (C.3) is denoted by $\mathscr{U}$ when considering the nonlinear dynamics.

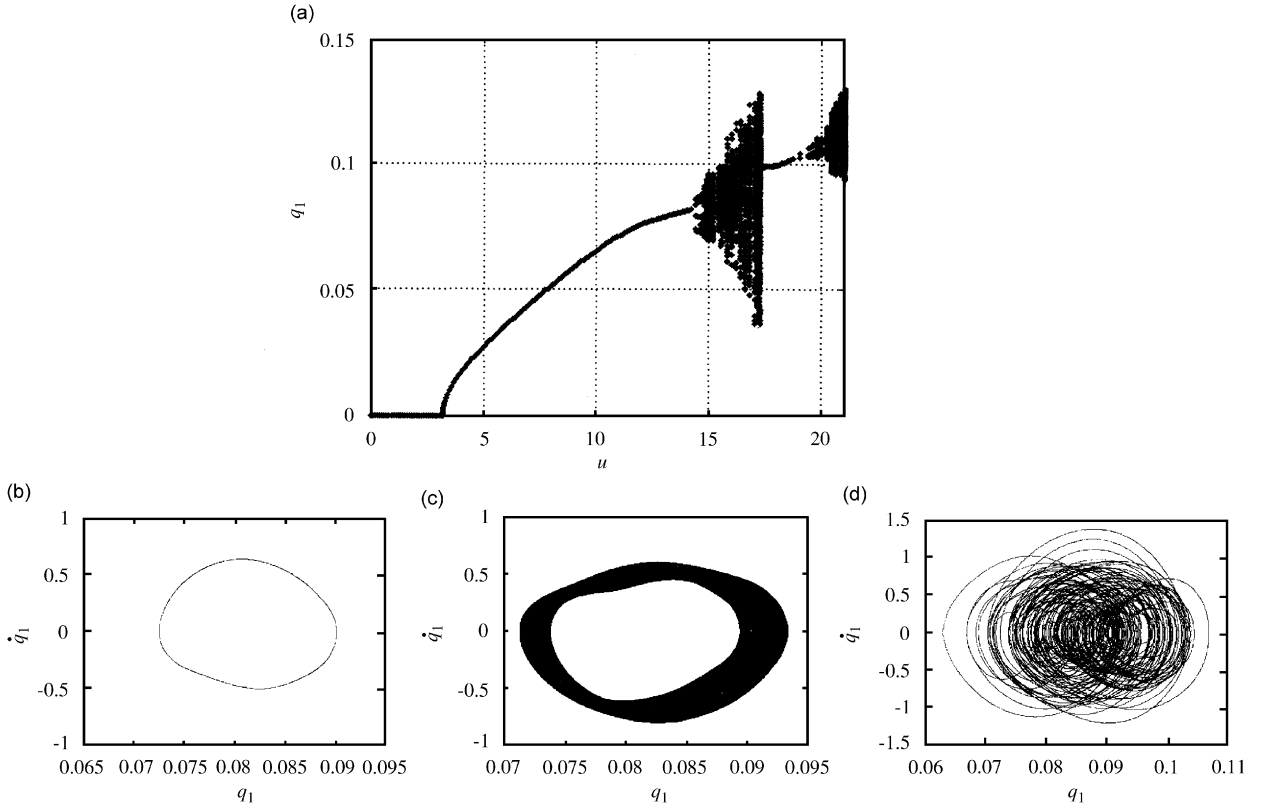

Fig. 7. (a) Bifurcation diagram for a simply supported cylinder in axial flow, showing the first Galerkin generalized coordinate q_1 versus the dimensionless flow velocity $\mathscr{U}$, representative of the overall system behaviour, for example for $\eta(0.4,\tau)$, for $\beta = 0.47, \gamma = 0.838, c_n = c_t = 0.025, \varepsilon = 15.81, \delta = 1, \nu = 0.47,\ \Pi_0 = 4000, \chi = 1, \overline{\Pi} = \overline{\Gamma} = c_b = c_d = 0$, obtained with six Galerkin modes each in the axial and transverse directions. Phase-plane portraits at (b) $\mathscr{U} = 14.6$, (c) $\mathscr{U} = 14.8$, and (d) $\mathscr{U} = 16$. From Ref. [32].

Naturally, the existence of post-divergence flutter in the second (and third) mode comes into question. However, in this case also, they do materialize; see, e.g., Fig. 9(b) for a horizontal system, and Ref. [4, Fig. 8.19] for a vertical one. The work done by the fluid forces in the course of a period of oscillation is found [4] to be

$$\begin{aligned}\Delta W = & -(1-f)MU\int_0^T [\dot{y}^2 + U\dot{y}y']_L \,\mathrm{d}t + \frac{1}{2}MU^2 c_b \int_0^T [\dot{y}y']_L \,\mathrm{d}t \\ & -\frac{1}{2}c_N(MU/D)\int_0^T\int_0^L (\dot{y}^2 + U\dot{y}y')\,\mathrm{d}x\,\mathrm{d}t - \frac{1}{2}(M/D)\int_0^T\int_0^L (c^*\dot{y}^2 - c_T U^2 \dot{y}y')\,\mathrm{d}x\,\mathrm{d}t \end{aligned} \tag{8}$$

in this case; here the overdot and prime denote, respectively, $\partial(\ )/\partial t$ and $\partial(\ )/\partial x$. The energy transfer is generally dominated by the terms on the first line of Eq. (8). It is seen that, in this case, if $f = 0$ the work done by the inviscid forces is maximized and, indeed, the first term becomes identical to Eq. (4). This, however, contradicts the experimental observation, oft repeated, that a cylinder with a blunt end does not flutter at all! The paradox is resolved by considering the second term. If the end is blunt, the form drag would be maximum, and this term would greatly diminish or totally eclipse the all-important second component of the first term.

The dynamics of the system has been re-examined theoretically, by means of nonlinear theory, and experimentally [35–37]. It was found that the dynamical behaviour, *grosso modo*, is as predicted by linear theory, though the bifurcations do not arise in the same way. A typical bifurcation diagram, Fig. 10, (in terms of the first component in the Galerkin-type solution, which nevertheless captures the dynamics), shows that, after divergence, there is a brief restabilization prior to the onset of second-mode flutter, as predicted by linear

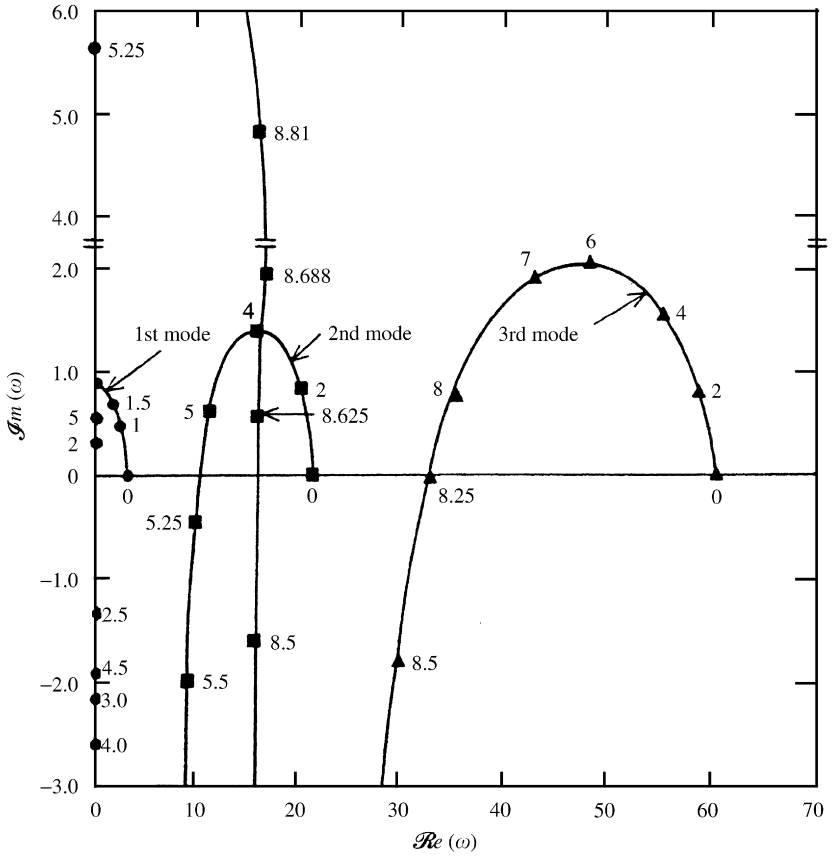

Fig. 8. Argand diagram of the complex eigenfrequencies, ω, of the lowest three modes of a solitary cantilevered cylinder with a tapered free end in unconfined axial flow, as functions of u, for $\beta = 0.5, \varepsilon c_f = 1, \delta = 0, \chi = 1, f = 0.8, \chi_e = 0.01, c_b = \gamma = 0$; from Ref. [29].

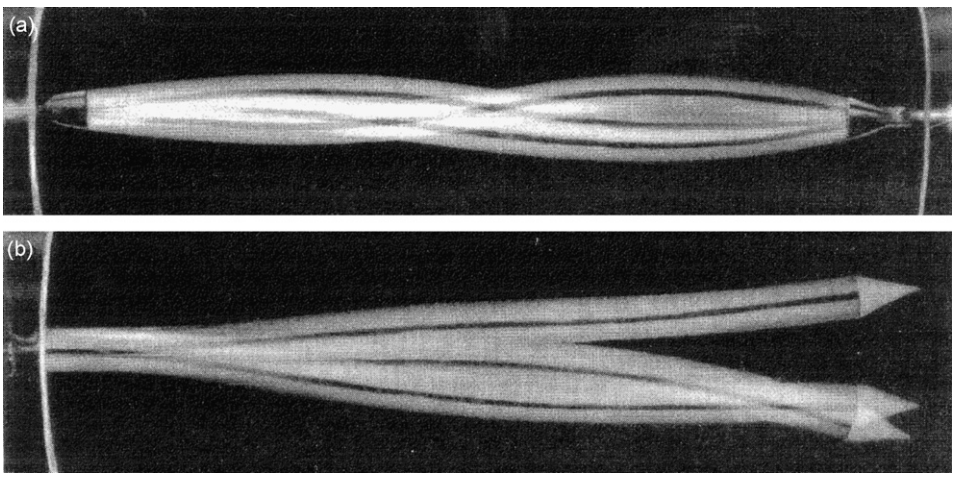

Fig. 9. Photographs of flexible cylinders in axial flow undergoing second-mode flutter: (a) a pinned–pinned cylinder; (b) a cantilevered one; from Ref. [31].

theory. Third-mode flutter, however, emanates from the second-mode solution branch, rather than from equilibrium. Agreement between nonlinear theory and experiment was quite good [26], both qualitatively (Fig. 11) and quantitatively.

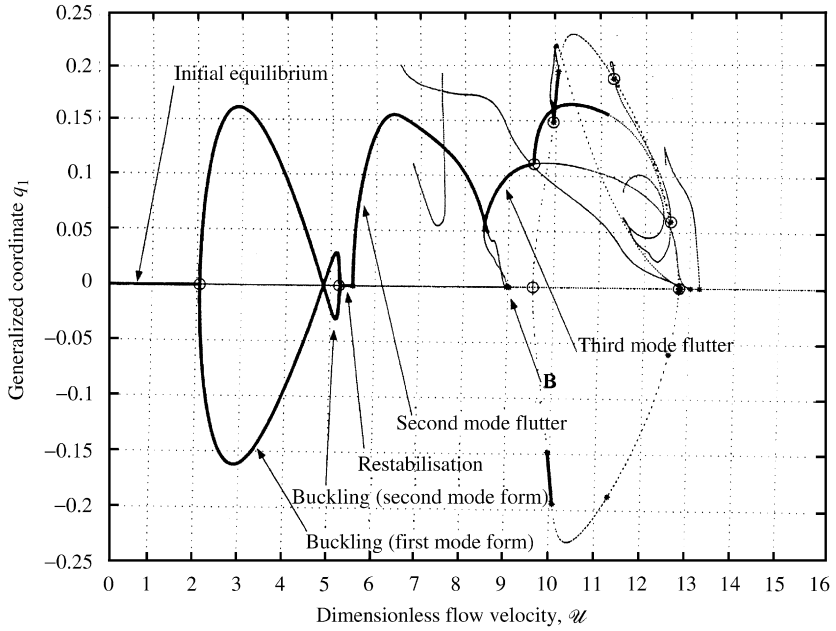

Fig. 10. Typical bifurcation diagram for $\beta = 0.47$, $f = 0.7$, $\gamma = 1.9$, $\varepsilon c_N = \varepsilon c_T = 0.5$, $c_b = 0.3$, $\chi_e = 0.00667$, $\overline{\chi}_e = 0.00785$, $c_d = 0$, $\chi = 1$ and $h = 0$, with $N = 6$ (for $\mathscr{U} < 9$) and $N = 8$ modes in the Galerkin approximation, showing the first generalized coordinate, q_1, as a function of $\mathscr{U}$: —, stable solutions; —, ···, unstable solutions; from Ref. [37].

A considerable amount of work (1996–2000) has been conducted on towed cylinders. The system under consideration is shown in Fig. 12. The dynamics in this case is complicated by the presence of rigid-body modes as well, thanks to the upstream end being unsupported also, albeit constrained by the towrope. For an extensive discourse, refer to Ref. [4, Section 8.9]. Briefly, however, the low towing-speed dynamics is dominated by rigid-body instabilities (e.g. divergence, or "criss-crossing" oscillations in which the cylinder and the towrope oscillate 180° out-of-phase). At higher towing speeds flexural instabilities arise, much as for a cantilevered cylinder. In this case, however, in addition to the tail-end shape, the "nose" shape and the towrope-length/cylinder-length ratio are important parameters.

An important application of this work (Section 3.4) is for very long and slender systems ($\varepsilon = L/D \sim \mathscr{O}(10^3)$). However, Dowling's [38] finding that systems with ε larger than a certain value are unconditionally immune to flutter put a damper on further work. Here it is of special interest to remark on the existence of a critical point along the long cylinder where the effective compressive force associated with the second term in Eq. (5) is nullified by the fifth term (representing cumulative tension induced by the longitudinal drag); indeed, ahead of this point the dynamics is dominated by the tension/compression effects (the terms proportional to $\partial^2 y/\partial x^2$), whereas downstream of that point flexural forces cannot be ignored. In fact, if one considers that a large portion of the forward part of the cylinder is effectively rigidified by the cumulative drag, there still remains the downstream part which should behave much like a shorter cylinder in axial flow [39]; indeed, there have been experiments suggesting that oscillatory instabilities do occur for long cantilevers subjected to axial flow, with the oscillations being confined to a small portion near the free end [40].

It is clear that the above constitute yet another paradox. It was resolved only recently by de Langre et al. [41]. It was found that Dowling's sophisticated analysis proved the non-existence of flutter by presuming it to arise via a Hopf bifurcation. If one relaxes this requirement and accepts the possibility that it may arise as a coupled-mode flutter of the Païdoussis type (as in Figs. 1 and 6), then flutter is indeed found to exist.

3.2. Clustered cylinders

The dynamics of clustered cylinders in axial flow has received considerable attention [42,4, Chapter 9] because such systems exist in many engineering applications (Section 3.4).

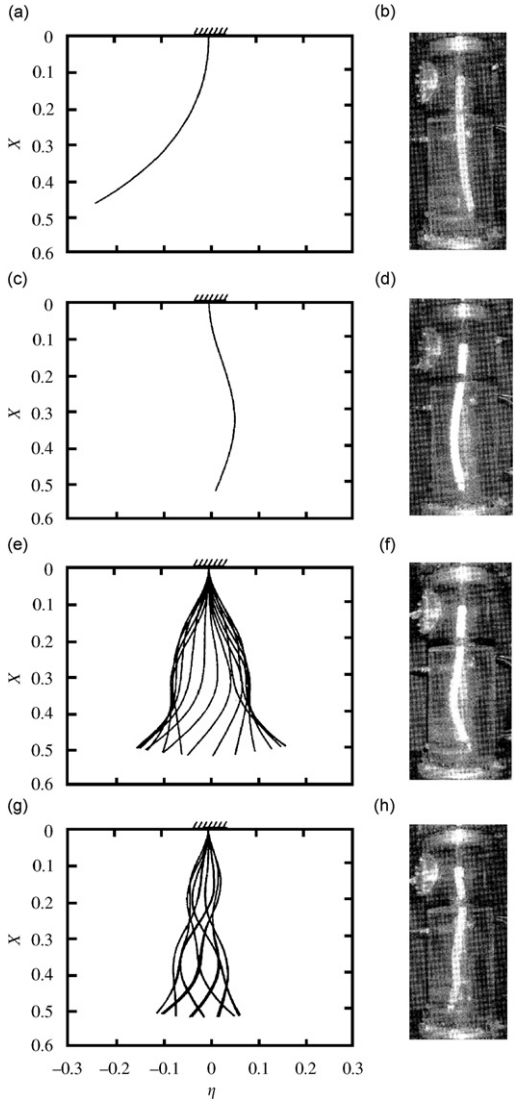

Fig. 11. Shape of the cylinder: qualitative comparison between theory (a, c, e, g) and experiment (b, d, f, h) showing successively: buckling of first-mode shape, buckling of second-mode shape, second-mode flutter, and third-mode flutter; from Ref. [37].

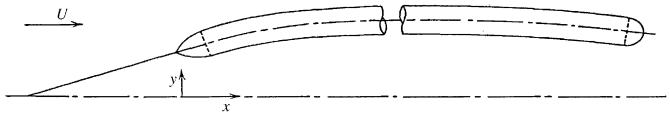

Fig. 12. Idealized system of a towed cylinder with non-cylindrical "nose" and "tail" segments, from Ref. [54].

What differentiate the dynamical behaviour of such systems *vis-à-vis* that of isolated cylinders are (i) the effect of *proximity* of the other cylinders which causes the various instabilities to occur at lower flow velocities, and (ii) the effect of inter-cylinder motion *coupling*, which further diminishes the critical flow velocities. Indeed, the latter effect means that a cluster of four cylinders possesses eight coupled modes of first flexural-mode shape rather than just one. This results in bands of flow velocities over which instabilities occur, as shown for instance in Fig. 13. Each of the modes shown involves a different

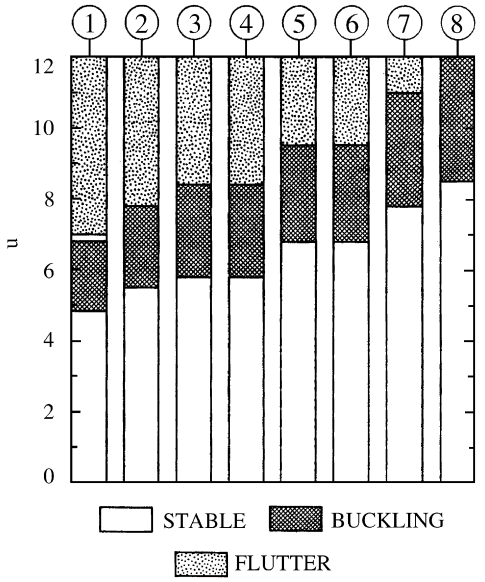

Fig. 13. Regions of stability and instability for a typical four-cylinder cluster when considering the whole of the first flexural-mode group. (Note that other instabilities arising from the second flexural-mode group also exist, starting from $u = 9.55$, but are not shown for clarity.) From Ref. [43].

"cross-sectional", i.e. inter-cylinder modal pattern. Some experimentally observed patterns of divergence and flutter of three- and four-cylinder clusters are shown in Fig. 14.

The interested reader is referred to the aforementioned references for a wealth of interesting dynamics on this topic.

3.3. Links with the work on pipes conveying fluid

If one follows the development of the work related to the dynamics of cylinders in axial flow in the references cited, it becomes crystal clear that the understanding of the dynamics, the energy transfer considerations, methods of solution, and to some extent the experimental techniques, all owe a great deal to the earlier studies on the dynamics of pipes conveying fluid.

3.4. Applications

The very first studies on the dynamics of cylinders in axial flow were motivated by application to the vibration of fissile fuel rods in nuclear reactors [44]. They led to a still-used semi-empirical relation for predicting the turbulence-induced vibration levels in such systems [45,46].

The first study on the dynamics of towed flexible cylinders was conducted by Hawthorne [30] in conjunction with his invention of the Dracone barge for the transportation of lighter than sea-water cargo, such as oil or fresh water, towed behind a small boat.

Further research, however, was mainly curiosity driven. Nevertheless, many applications have emerged as follows:

(i) dynamics of control rods and reactivity monitors in nuclear reactors [47];
(ii) dynamics of extruding metal and plastic rods in liquid [48,49];
(iii) sophisticated codes for prediction of vibration in closely spaced clusters of cylinders [50,51];
(iv) dynamics of nuclear reactor strings (or "stringers") [4];
(v) the turbulence-induced vibration of tube arrays in heat exchangers (in the zones where the flow is mainly axial) [52,53];

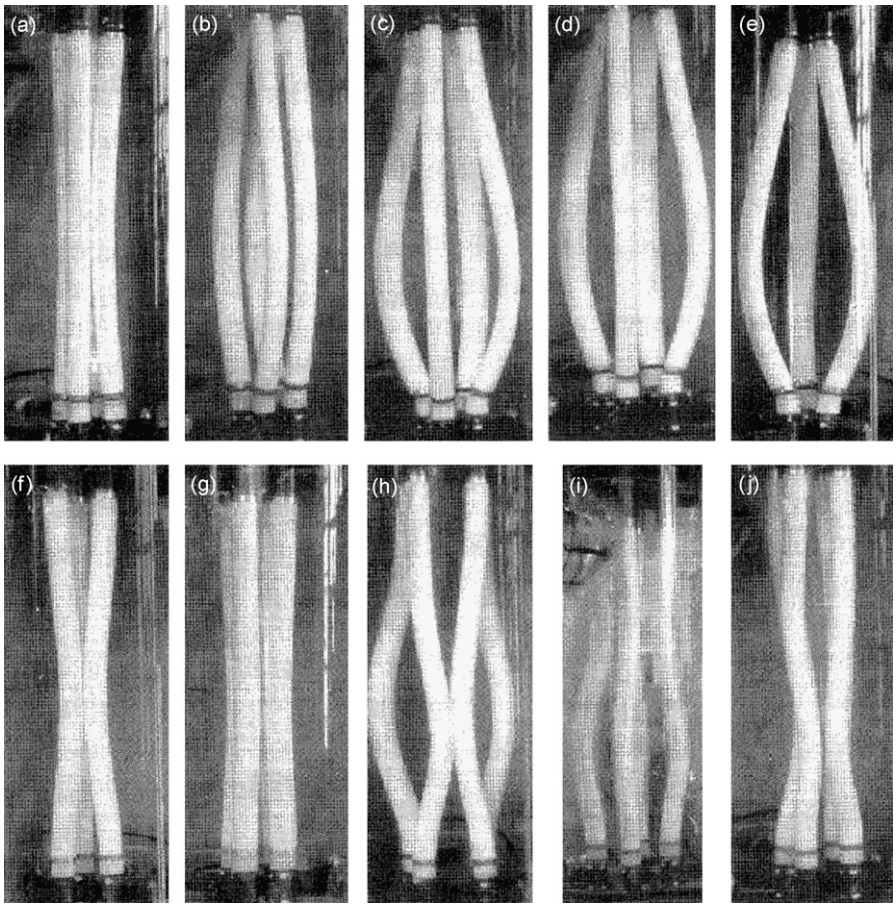

Fig. 14. Photographs of four- and three-cylinder systems, with cylinders made of elastomer, either (a)–(e) pinned, or (f)–(j) clamped at both ends—but free to slide axially at the downstream end. (a) $K=4,\ G_c=1,\ u=2.86$ ($U=1.74\,\mathrm{m/s}$); (b) $K=4,\ G_c=1,\ u=3.40$ ($U=1.94\,\mathrm{m/s}$); (c) $K=4,\ G_c=1,\ u=4.77$ ($U=2.55\,\mathrm{m/s}$); (d) $K=4,\ G_c=3,\ u=4.16$ ($U=2.37\,\mathrm{m/s}$); (e) $K=3,\ G_c=1,\ u=4.55$ ($U=2.77\,\mathrm{m/s}$); (f) $K=3,\ G_c=2,\ u=5.46$; (g) $K=4,\ G_c=1,\ u=4.87$; (h) $K=4,\ G_c=3,\ u=8.24$; (i) $K=4,\ G_c=3,\ u=7.20$; (j) $K=4,\ G_c=2,\ u=9.42$. From Ref. [43].

(vi) stability and vibration of extremely long "acoustic arrays" (or "seismic arrays"), towed behind boats and used in oil and gas exploration in the high seas [38,54–56];
(vii) the dynamics of towed pipelines for easy relocation where they are needed in the ocean [57];
(viii) the dynamics of articulated submarine transporters [58,4];
(ix) wire coating and fibre spinning [59–62];
(x) high-speed trains travelling in tunnels [63,64].

This work has also provided the fundamental understanding for the analysis of other systems, e.g. the fluidelastic instabilities in annular and leakage flows [4, Chapter 11].

4. Dynamics of cylindrical shells subjected to axial flow

4.1. General dynamical behaviour

Consider a cylindrical shell either containing a flowing fluid or immersed in an axial flow.

The linear equations of motion may be written in the following form [65,4]:

$$\mathscr{L}_1(u,v,w)=\gamma\frac{\partial^2 u}{\partial t^2},\quad \mathscr{L}_2(u,v,w)=\gamma\frac{\partial^2 v}{\partial t^2},\quad \mathscr{L}_3(u,v,w)=-\gamma\left[\frac{\partial^2 w}{\partial t^2}-\frac{q_r}{\rho_s h}\right], \tag{9}$$

where the left-hand sides are linear differential operators of the axial coordinate x and the circumferential (azimuthal) angle θ; u, v and w are, respectively, the axial, circumferential and radial displacements of the middle surface of the shell (Fig. 15). In Ref. [65] Flügge's equations for thin shells were used, thus presuming small thickness-to-radius ratios, h/a, but equivalent ones may be found, e.g., in Ref. [66]. Eqs. (9) are given in full in Appendix D. In the last equation, q_r is the radial surface loading per unit area, defined in terms of the internal and external pressures on the shell, p_i and p_e, by

$$q_r=p_i-p_e. \tag{10}$$

The fluid is assumed to be inviscid and incompressible for simplicity and the flow irrotational; and p_i and p_e are supposed to be composed of mean steady components and the shell-deformation-related perturbation components. The effect of the steady components is ignored here, for simplicity.

Considering $\{u,v,w\}^{\mathrm{T}}=\{A,B,C\}^{\mathrm{T}}\exp[\mathrm{i}(\lambda x/a+n\theta+\Omega t)]$ and a velocity potential for the fluid $\Phi=R(r)\exp[\mathrm{i}(\lambda x/a+n\theta+\Omega t)]$, the perturbation components may be obtained via potential flow theory [65] and are found to be

$$p_i^*=-\rho_i\frac{a}{n+\lambda I_{n+1}(\lambda)/I_n(\lambda)}\left[\frac{\partial}{\partial t}+U_i\frac{\partial}{\partial x}\right]^2 w,$$

$$p_e^*=-\rho_e\frac{a}{n-\lambda K_{n+1}(\lambda)/K_n(\lambda)}\left[\frac{\partial}{\partial t}+U_e\frac{\partial}{\partial x}\right]^2 w, \tag{11}$$

at $r=a-0^+$ and $r=a+0^+$, respectively, for $h/a\ll 1$. Here ρ_i and ρ_e are the fluid densities of the internal and external fluids, respectively, U_i and U_e are the corresponding flow velocities, λ is the axial wavenumber, and n is the circumferential wavenumber; if the internal or external fluid is quiescent, Eqs. (11) still apply but with either U_i or U_e equal to zero.

It is interesting to note that the terms arising from the square-brackets operator in Eq. (11) are $\partial^2 w/\partial t^2$, $U^2(\partial^2 w/\partial x^2)$ and $2U(\partial^2 w/\partial x\partial t)$. These terms are associated, respectively, with the inertia of the fluid, and the centrifugal and Coriolis forces of the moving fluid. Thus, the fluid loading is wholly analogous to that acting on a tubular beam conveying fluid, as discussed in Section 2. It is, therefore, not surprising that the

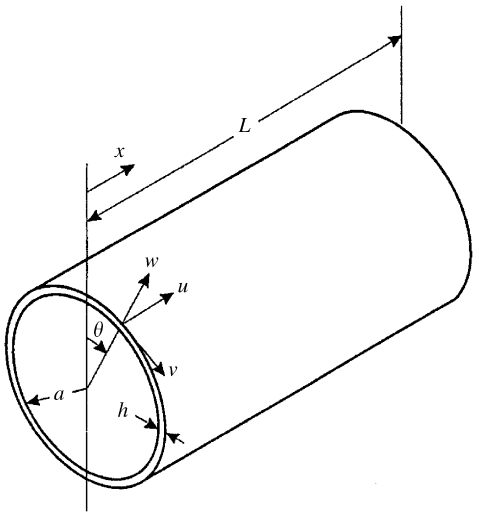

Fig. 15. A cylindrical shell, showing the coordinate system and some key dimensions.

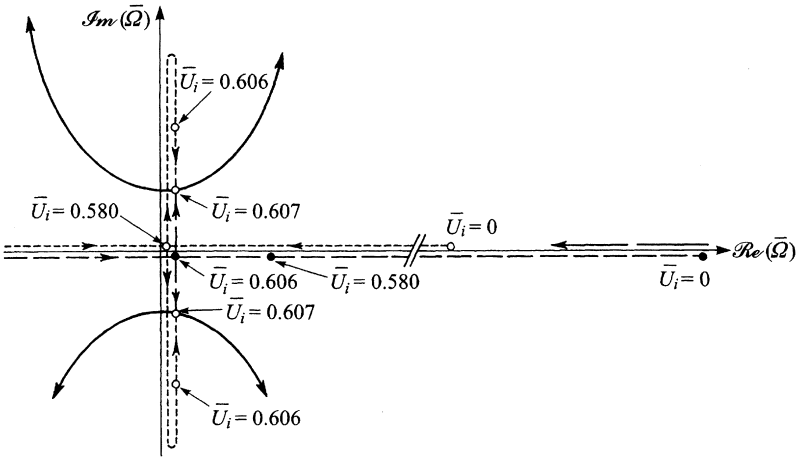

Fig. 16. Argand diagram of the dimensionless frequency, $\overline{\Omega}$, as a function of $\overline{U}_i$ for a clamped–clamped shell; $n = 2$, and $h/a = 2.27 \times 10^{-2}, L/a = 25.9, \nu = 0.50, \mu_i = \mu_e = 0.06$. The loci on the real and imaginary axes have been drawn slightly off the axes but parallel to them for clarity. – – –, $m = 1$; — — —, $m = 2$; ——, combined $m = 1$ and $m = 2$; —— ——, $m = 3$. From Ref. [65].

basic dynamical behaviour of the system is quite similar to that of a pipe conveying fluid, as shown in Figs. 16 and 17 for a clamped–clamped shell and a cantilevered shell, in both cases subjected to internal flow.

The dimensionless flow velocity, frequency and mass parameter are defined by

$$\overline{U}_f = \left[\frac{\rho_s(1-\nu^2)}{E}\right]^{1/2} U, \quad \overline{\Omega}_f = \left[\frac{\rho_s(1-\nu^2)}{E}\right]^{1/2} a\Omega, \quad \mu_f = \frac{a}{h}\frac{\rho_f}{\rho_s}, \tag{12}$$

where f is either i or e, E is Young's modulus for the shell, ρ_s the shell material density and ν the Poisson ratio.

It is seen in Fig. 16 that the system loses stability by divergence in its second circumferential mode ($n = 2$) and first axial mode ($m = 1$)[4] at a dimensionless flow velocity $\overline{U}_i = 0.580$, and in the second axial mode ($m = 2$) at $\overline{U}_i = 0.606$. Immediately after, the first and second-mode loci coalesce, and coupled-mode flutter is predicted at $\overline{U}_i = 0.607$. Similar dynamics is predicted for other n. Once again, the reliability of the post-divergence predictions by linear theory is questionable and needs to be re-examined by means of nonlinear theory, as discussed later.

In Fig. 17, it is seen that the cantilevered system loses stability by a Hopf bifurcation in the $n = m = 2$ mode at $\overline{U}_i \simeq 0.45$ and in the $n = 3, m = 2$ mode at $\overline{U}_i \simeq 0.5$. Thus, again, the dynamics is quite similar to that of a pipe conveying fluid.

The dynamics with external flow is quite similar to that shown in Figs. 16 and 17.

Experiments with elastomer shells and air-flow showed that cantilevered shells lose stability by flutter, as predicted by theory [65,67]. In the case of shells with clamped ends, however, the dynamics with internal and external (actually, annular flow, externally contained by an outer rigid pipe) was different: with external flow the system lost stability by divergence, while with internal flow the system *lost* stability by flutter [65,68]. At the time, this discrepancy was supposed to be related to the proximity of the divergence and coupled-mode flutter boundaries (cf. Fig. 16). Later, it was theorized that this may be a case of oscillatory divergence, associated with the large amplitudes of deflections involved in the elastomer shells.

Hence, it was clear that re-examination of the system dynamics was necessary, with the following two goals: to clarify (i) the non-occurrence of divergence in the experiments and (ii) the predicted coupled-mode flutter by linear theory. Clearly, therefore, this re-examination must involve both nonlinear theory and further experiments. This is discussed in greater detail by Karagiozis et al. [69–71] and Païdoussis [72].

[4] m is the number of half-waves in the axial domain $[0, L]$, L being the length of the shell.

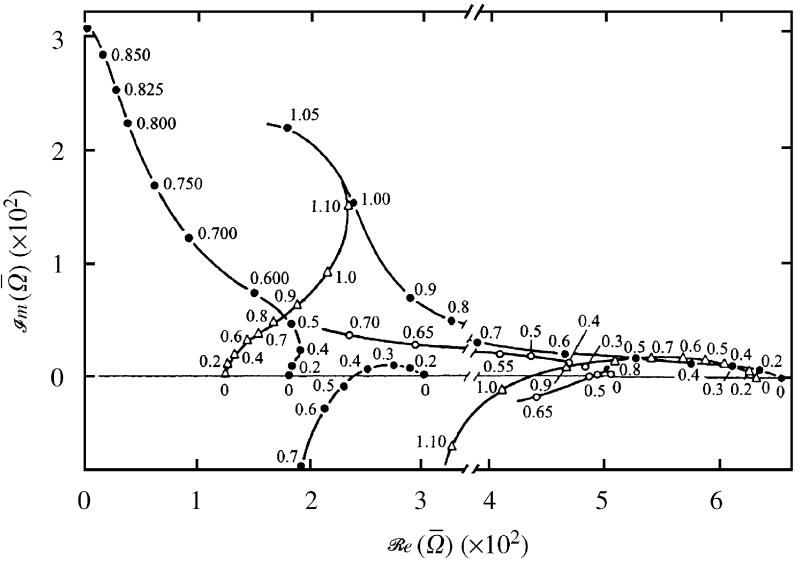

Fig. 17. Argand diagram of the dimensionless frequency, $\overline{\Omega}$, as a function of the dimensionless flow velocity, $\overline{U}_i$, for a cantilevered shell; $h/a = 2.27 \times 10^{-2}$; $L/a = 12.9, \nu = 0.50, \mu_i = \mu_e = 0.06$, showing the first two axial modes, $m = 1$ and 2, for $n = 1, 2, 3$, as well as the $n = 2, m = 3$ mode: $\Delta, n = 1$; $\bullet, n = 2$; $\circ, n = 3$. From Ref. [65].

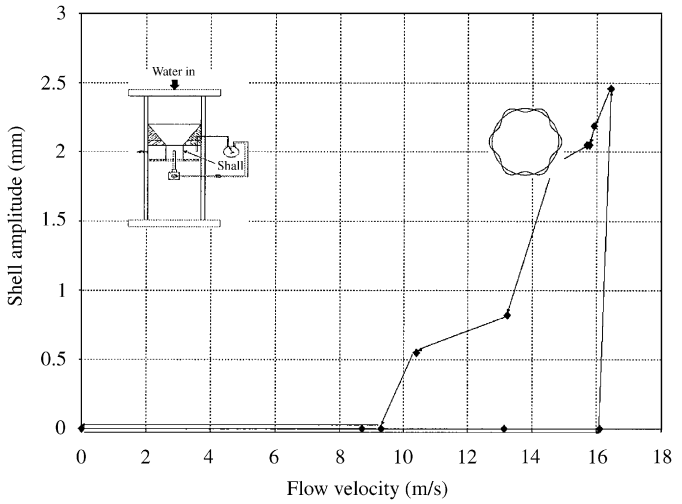

Fig. 18. The amplitude versus flow velocity diagram for an aluminium shell ($L/R = 2.98$) subjected to internal water-flow and inwards intramural pressurization; $\Delta P_{tm}(x) = P_{\text{ann}} - P_{\text{inn}}(x) > 0$ and $P_{\text{ann}} - P_{\text{inn}}(L/2) = 5.7\,\text{kPa}$. From Ref. [69].

First, the question of non-occurrence of divergence in the internal flow experiments was resolved [72,73] by conducting experiments with stiffer (aluminium or plastic) shells, in which motions were of the order of the shell thickness, instead of being of the order of the shell radius as with elastomer shells. It was found that the stiffer shells did indeed lose stability by divergence, as shown in Figs. 18 and 19, as predicted by theory. Hence, the supposition of oscillatory divergence for the more pliable shells was also given indirect support.

With this reconciliation between theory and experiment as to the mode of loss of stability of shells with supported ends subjected to internal flow, the question of existence of coupled-mode flutter at higher flows can meaningfully be addressed. In fact, the answer to that one was already available. The nonlinear theory of Amabili et al. [74] for shells with simply supported ends conveying fluid predicts that they lose stability by

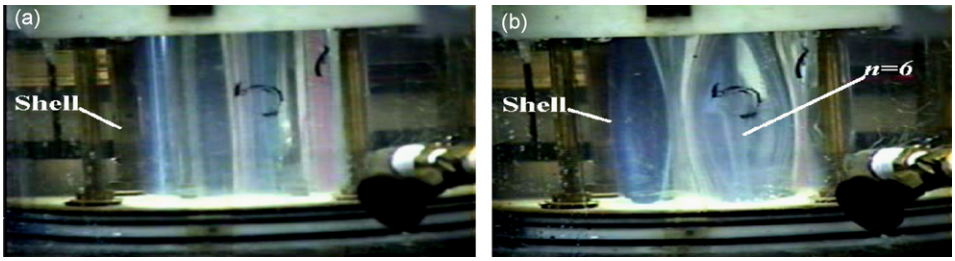

Fig. 19. The aluminium shell in internal water-flow: (a) before instability and (b) when divergence has occurred. The vertical striations in (a) are reflections of the incident light; note that in (b) they are no longer straight. (Note: these photographs are not from the same experiment as that of Fig. 18.) From Ref. [69].

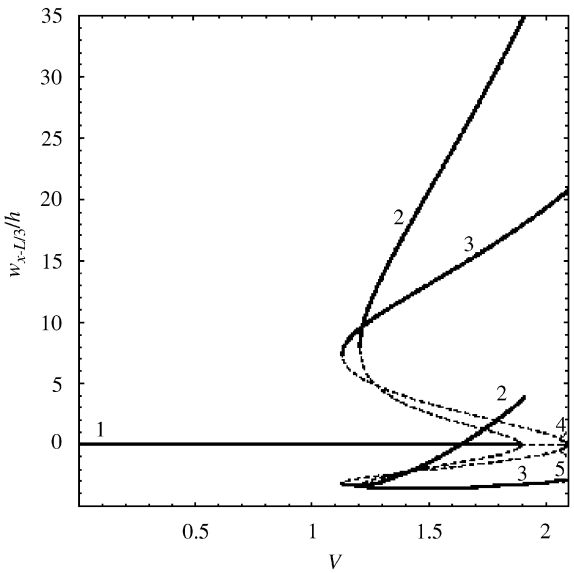

Fig. 20. Shell amplitude versus the nondimensional flow velocity of a clamped PET shell with internal water-flow, V, at $x = L/3$ and $\theta = 0$. ——, Stable solution branches: — —, unstable solution branches; 1, solution Branch 1; 2, solution Branch 2; 3, solution Branch 3; 4, solution Branch 4; 5, solution Branch 5. From Ref. [70].

divergence via a strongly subcritical pitchfork bifurcation, but that they do not develop coupled-mode flutter. However, as the experiments [69] were always done with shells with clamped ends (for experimental convenience), to close the file on this issue a new nonlinear theoretical model was developed for shells with clamped ends [70,71]; see Appendix D. The predictions are similar to those of simply supported shells: loss of stability by strongly subcritical divergence and no subsequent flutter. A typical result is shown in Fig. 20. Theory and experiment are in reasonable agreement with each other quantitatively also.

Thus, with the recent (1999–2006) work on this subject, the dynamics of shells conveying fluid or immersed in axial flow has been shown to be quite similar to that of pipes conveying fluid. Indeed, if the radial shell deformation is expressed as $w(x,\theta,t) = \overline{w}(x)\cos n\theta$, the work done by the fluid on the shell during a cycle oscillation may be written as

$$\Delta W = -\rho\pi a^2 \mathscr{I}(n,\lambda) U \int_0^T \left[\left(\frac{\partial \overline{w}}{\partial t}\right)^2 + U\left(\frac{\partial \overline{w}}{\partial x}\right)\left(\frac{\partial \overline{w}}{\partial t}\right) \right]_0^L \mathrm{d}t, \tag{13}$$

where ρ is the fluid density, U the flow velocity, a and L the shell radius and length, respectively, and $\mathscr{I}(n,\lambda)$ a functional of Bessel functions dependent on the circumferential and axial wavenumbers, n and m, respectively.

Hence, the same conclusions hold as for a pipe conveying fluid. For the shell with both ends supported, $\Delta W = 0$, and, as shown by nonlinear theory also, the predictions of post-divergence coupled-mode flutter by linear theory are incorrect. For cantilevered shells, flutter does materialize and the form of Eq. (13) being similar to Eq. (2) implies that for flutter the free-end velocity and slope must be in quadrature, which in fact is what is observed—see, e.g., Ref. [65].

All the foregoing work presumes that the dynamics may be adequately predicted by assuming the fluid flow to be inviscid. Moreover, unlike the problem of the fluid-conveying pipe, here friction-related forces do not cancel out, except for $n = 1$ (i.e. for beam-like motions). Generally speaking, it was found that, if the shell is not short (i.e., for L/a not too small), the steady viscous effects, manifested as a variable mean pressure inside the shell and to a smaller extent surface traction, are not negligible; see Appendix D. Thus, if the mean pressure within the shell, as a result of viscous pressure loss, becomes lower than the outside ambient pressure, the shell is destabilized. Unsteady viscous effects, again generally, have been found to be less important. For details, the reader is referred to Ref. [4, Chapters 7 and 11].

Also, in all the foregoing the fluid flow was presumed to be incompressible or at least subsonic. There is an enormous amount of work on compressible, supersonic or transonic flows in contact with cylindrical shells, particularly because of its application to high-speed aircraft, missiles and space vehicles. The interested reader is referred to Dowell's work [75,76].

4.2. Confinement effects and annular flows

If the shell is placed within a cylinder or another shell and subjected to either internal flow or flow in the annulus, or both, the dynamics becomes more complex. For one thing, if the fluid in the annulus is dense, because the shell is very thin the natural frequencies are strongly affected by large added mass effects. Also, the critical flow velocities are generally diminished by confinement, and more so by fluid-dynamic coupling in the case of coaxial shells. The dynamics, nevertheless, remains broadly similar to that described in Section 4.1, and hence fundamentally similar to the dynamics of a pipe conveying fluid [4, Chapters 7 and 11].

4.3. Applications

Direct or indirect applications of this work are numerous. Thin-walled shells are used in piping in aircraft and space vehicles, penstrocks in hydroelastic plants, nuclear reactors (thermal shields), aircraft engines, submerged pipelines, shell-type Coriolis flow meters, heat exchangers, and many other systems.

Also, considering large-amplitude motions of the type already encountered in the foregoing when discussing experiments with elastomer shells, the similarity of the basic dynamics to that of very pliable, *collapsible tubes* studied for physiological application to arteries, veins, pulmonary and urinary passages is easily appreciated, at the physical level; although much of the analytical work followed another path, more appropriate for the very large shell deformations involved [77,78; 4, Section 7.9]. This is a huge topic on its own, and in a paper such as this it can only be touched upon.

It is obvious, however, how much wider the range of engineering and physiological applications has become, *vis-à-vis* that of the pipe conveying fluid.

5. Dynamics of plates in axial flow

5.1. General dynamical behaviour

Consider a two-dimensional plate (i.e. one of essentially infinite width) of flexural rigidity $\mathscr{D} = Eh^3/[12(1-\nu^2)]$, E and ν being the same as elsewhere and h the plate thickness, and density ρ_p, subjected to a flow-related perturbation pressure p^*. The linear equation of motion is

$$\mathscr{D}\frac{\partial^4 w}{\partial x^4} + C_d\frac{\partial w}{\partial t} + \rho_p h\frac{\partial^2 w}{\partial t^2} = -p^*, \tag{14}$$

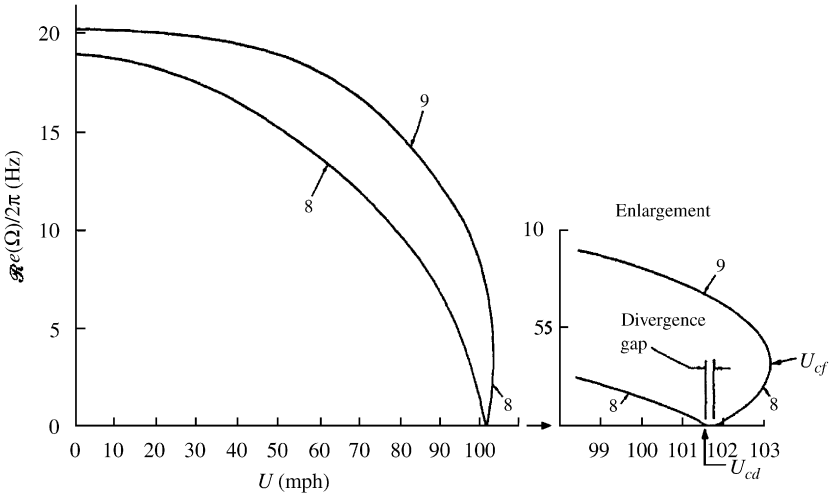

Fig. 21. Frequencies of free oscillation, $\mathrm{Re}(\Omega)/2\pi$, versus flow velocity for the two-mode analysis of Dugundji et al., showing the eighth and ninth modes, and the critical flow velocities for divergence, U_{cd}, and flutter, U_{cf}, in mph (miles/h); 1 mph = 1.609 km/h = 0.447 m/s. From Ref. [81].

in which C_d is a viscous damping coefficient. Assuming the flow to be inviscid, the complete solution for p^* has been obtained by Kornecki et al. [79]

$$-p^* = \frac{\rho}{\pi L}\left\{\int_0^1 \left[L^2\frac{\partial^2 w}{\partial t^2} + 2UL\frac{\partial^2 w}{\partial \xi \partial t} + U^2\frac{\partial^2 w}{\partial \xi^2}\right]\ln|\overline{x}-\xi|\mathrm{d}\xi - R(\overline{x})\right\}, \tag{15}$$

where

$$R(\overline{x}) = U^2\{[w'(1) + (L/U)\dot{w}(1)]\ln(1-\overline{x}) - [w'(0) + (L/U)\dot{w}(0)]\ln\overline{x}\}, \tag{16}$$

in which $\overline{x} = x/L$ and $\xi = u/L, u$ being a dummy variable; t is dimensional time, and $(\dot{\ }) = \partial(\ )/\partial t$, while $(\ )' = \partial(\ )/\partial\overline{x}$; ρ is the fluid density.

The integrand on the right-hand side of Eq. (15) has the same functional form as in Eq. (1), and the function $\ln|\overline{x}-\xi|$ may be viewed as the effect of spatial memory. There is, however, a significant difference in the theories in Sections 2–4 and that for the plates here: for pipes, cylinders and shells the local fluid forces depend only on the local displacement,[5] while for the plate problem the local forces depend on the global flow field. Thus, for cylinders one has a constant added mass per unit length, and for shells the same (at least for any (n,λ) combination). For pipes conveying fluid, this is even clearer: the mass involved is the mass per unit length of the fluid conveyed. This is not so for the plate, as discussed further by Guo and Païdoussis [80]. Nevertheless, the dynamics of the plates in axial flow is quite similar to that in the foregoing.

Plates with supported ends lose stability by divergence and then, much as cylinders in axial flow, by coupled-mode flutter; see, e.g., Fig. 21. These theoretical findings were broadly supported by experiments conducted by Dugundji et al. [81].

Writing

$$\overline{U}^* = \left(\frac{\rho_p h}{\mathscr{D}}\right)^{1/2} UL, \quad \overline{U} = \overline{U}^*\mu^{1/2}, \tag{17}$$

where $\mu = \rho L/\rho_p h$, one finds the critical flow velocity for divergence to be

$$\overline{U}_{cd} = \alpha\pi, \tag{18}$$

with α varying from 1.00 to 1.40 depending on the approximations introduced [80–84; 4, Table 10.1].

[5]This is not necessarily physically true. It is, nevertheless, inherent in the approximate theories employed.

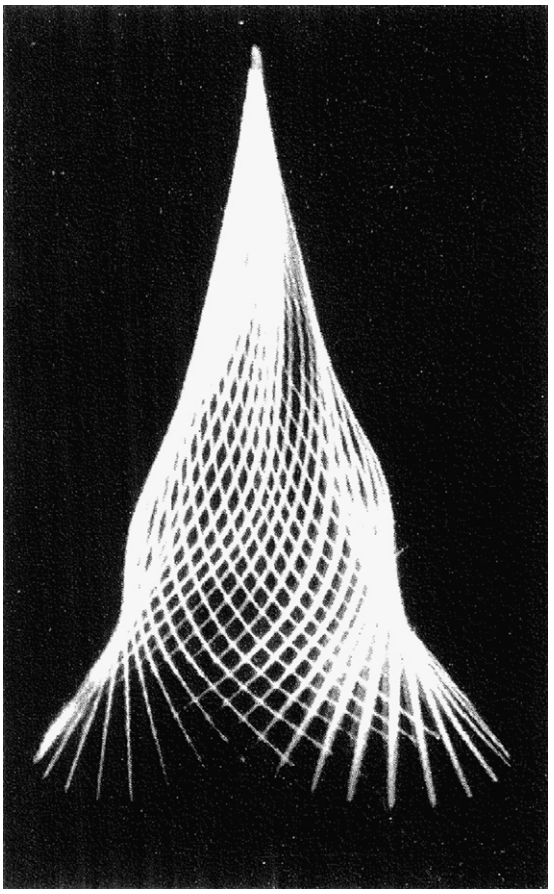

Fig. 22. Multiflash photograph of a fluttering sheet of paper $\mu^* = 2.70$; from Ref. [85].

In the case of cantilevered plates, the dynamics is much clearer: the system loses stability by flutter, as predicted by theory and observed experimentally (see, e.g., Fig. 22). The similarity in form of the fluttering plate to a fluttering pipe, in all its features, is quite remarkable. In this case, however, the prediction is complicated by the fact that, generally, the vorticity shed by the flapping plate into the wake should be taken into account [79,86,87].

Surprisingly, agreement between theory and experiment is not very good generally, although it is good in some cases. From Fig. 23 it is clear that agreement improves (but not for all data unfortunately) as $\mu \equiv 1/\mu^*$ is increased. This can be attributed to the effect of the wake on the plate dynamics becoming weaker for longer plates [87].

Much work has been done on this topic (work on three-dimensional plates in axial flow, in compressible and supersonic flows, nonlinear analyses, and so on), and what has been discussed here is a very small segment thereof, indeed. However, the purpose of this paper was to demonstrate the similarities and the implicit and explicit transfer of knowledge, understanding and so on, from the other systems discussed before, and this has been done—albeit in a much abbreviated fashion.

5.2. *Applications*

In this case, the premier example of a plate in axial flow is the fluttering flag. However, there is a profusion of technologically important applications [4, Chapter 10], e.g.:

(i) skins of aircraft, submarine and space vehicles;
(ii) parallel-plate assemblies used in some nuclear reactors;

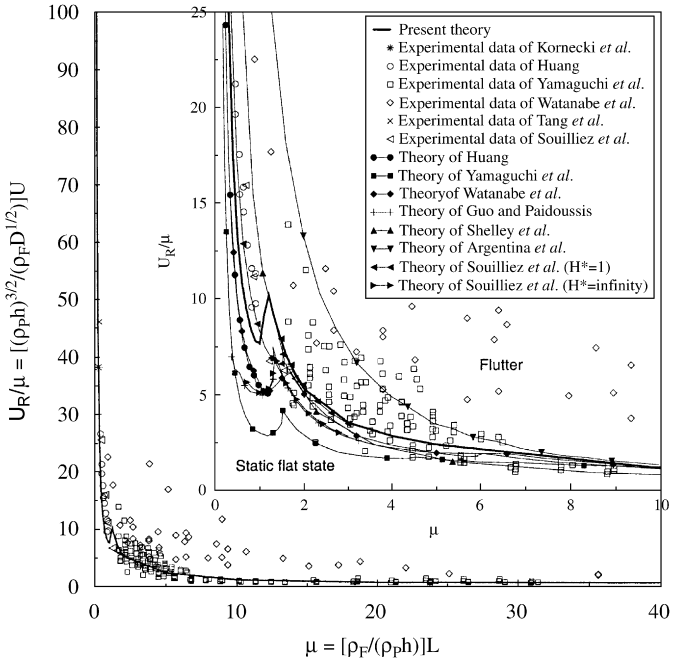

Fig. 23. The flutter boundary of cantilevered flexible plates in axial flow. For the results obtained using the "present theory" by Tang & Païdoussis, the system parameters used are: $l_0 = 0.01, \alpha = 0.004$ and $C_D = 0$; ρ_F is the fluid density. From Ref. [86].

(iii) modelling of pulmonary passages;
(iv) travelling web in paper and plastic tape production;
(v) printing, involving individual paper sheets;
(vi) studies on soft-palate-related snoring;
(vii) energy-harvesting foils.

6. Conclusion

While most of the basic work on the dynamics of pipes conveying fluid was being conducted, this was viewed as an academic study in Applied Mechanics, of little practical interest. The objective of this paper was to show how this work was used as the foundation in the study of many other related problems; hence the expression "radiation of the knowledge gained" in the title.

Indeed, the fundamental understanding and experience gained and the methodology employed in the study of the fluid-conveying pipe problem has proved to be very useful in the study of several other problems, particularly shells conveying or immersed in axial flow, cylinders and plates in axial flow, and (although discussed hardly at all in this paper, for brevity) annular and leakage flow problems—well known for their monumental destructiveness [47,88]. Other problems not discussed, a little farther in their nature from those mentioned above, have also benefited from the same methodology; an example is the study of ovalling oscillations of shells in cross-flow, with application to wind-induced ovalling of tall chimneys [88,89].

Throughout, both the similarities in the basic dynamics of the system considered, but also the differences, have been discussed.

There is no doubt that the great majority of the work on the many facets and modified versions of the basic system of a pipe conveying fluid were curiosity driven, with no practical motivation [28]. Nevertheless, as demonstrated in this paper by the ever-widening range of engineering and physiological applications (Sections 3–5), the effort expended in carefully studying pipes conveying fluid has been repaid many times over, not only from the fundamental point of view but in terms of applications as well. It was mentioned in the

Introduction that one can find at least 550 important contributions to the pipe-conveying-fluid problem; one can safely add 1500–2000 important studies in the "offshoots", equally if not more important!

Acknowledgements

The author gratefully acknowledges the support provided for this research by the Natural Sciences and Engineering Research Council (NSERC) of Canada and the Fonds québécois de la recherche sur la nature et les technologies (FQRNT) of Québec.

Appendix A

A.1. Other forms of the equation of motion of a pipe conveying fluid

If the pipe is subjected to an externally applied tension $\overline{T}$, internal pressurization $\overline{p}$, if it is vertically mounted so that gravity is operative, in contact with a Winkler-type elastic foundation of stiffness K, and moreover internal dissipation is taken into account by means of a Kelvin–Voigt model, as well as external viscous damping with the surrounding ambient fluid (with frictional coefficient c), the linear equation of motion—a generalization of Eq. (1)—is

$$\left(E^*\frac{\partial}{\partial t}+E\right)I\frac{\partial^4 w}{\partial x^4}+\left\{MU^2-\overline{T}+\overline{p}A(1-2v\delta)-\left[(M+m)g-M\frac{\mathrm{d}U}{\mathrm{d}t}\right](L-x)\right\}\frac{\partial^2 w}{\partial x^2}$$
$$+2MU\frac{\partial^2 w}{\partial x\partial t}+(M+m)g\frac{\partial w}{\partial x}+Kw+c\frac{\partial w}{\partial t}+(M+m)\frac{\partial^2 w}{\partial t^2}=0, \tag{A.1}$$

in which the flow velocity may not be steady; hence the $\mathrm{d}U/\mathrm{d}t$ term.

This equation may be written in the dimensionless form

$$\alpha\dot{\eta}''''+\eta''''+\{u^2-\Gamma+\Pi(1-2v\delta)+(\beta^{1/2}\dot{u}-\gamma)(1-\xi)\}\eta''$$
$$+2\beta^{1/2}u\dot{\eta}'+\gamma\eta'+k\eta+\sigma\dot{\eta}+\ddot{\eta}=0, \tag{A.2}$$

where the overdot stands for $\partial(\ )/\partial\tau$ and $(\ )'=\partial(\ )/\partial\xi$, in which the following dimensionless system parameters have been utilized:

$$\xi=\frac{x}{L},\quad \eta=\frac{w}{L},\quad \tau=\left[\frac{EI}{M+m}\right]^{1/2}\frac{t}{L^2},$$

$$u=\left(\frac{M}{EI}\right)^{1/2}LU,\quad \beta=\frac{M}{M+m},\quad \gamma=\frac{(M+m)L^3}{EI}g,\quad \Gamma=\frac{\overline{T}L^2}{EI},$$

$$\Pi=\frac{\overline{p}AL^2}{EI},\quad k=\frac{KL^4}{EI},\quad \alpha=\left[\frac{I}{E(M+m)}\right]^{1/2}\frac{E^*}{L^2},\quad \sigma=\frac{cL^2}{[EI(M+m)]^{1/2}}; \tag{A.3}$$

the dimensionless frequency ω is defined by

$$\omega=\left(\frac{M+m}{EI}\right)^{1/2}\Omega L^2, \tag{A.4}$$

where Ω is the radian frequency. Eq. (A.2) applies both to cases of pipes with supported ends and to cantilevered ones.

The boundary conditions are identical to those for a beam with the same support conditions.

The nonlinear equations of motion, however, are different for these two cases, because (i) in the case of a cantilevered pipe, a reasonable assumption is that the pipe centreline is inextensible, while (ii) in the case of supported ends, axial extension must be accounted for.

For a cantilevered pipe, the dimensionless nonlinear equation is given by

$$\begin{aligned}
&\alpha\dot{\eta}'''' + \eta'''' + \ddot{\eta} + 2\mathscr{U}\sqrt{\beta}\dot{\eta}'(1+\eta'^2)\\
&\quad + \eta''\left[\mathscr{U}^2(1+\eta'^2) + (\dot{\mathscr{U}}\sqrt{\beta}-\gamma)(1-\xi)\left(1+\frac{3}{2}\eta'^2\right)\right]\\
&\quad + \gamma\eta'\left(1+\frac{1}{2}\eta'^2\right) + \left(1+\alpha\frac{\partial}{\partial t}\right)[\eta''''\eta'^2 + 4\eta'\eta''\eta''' + \eta''^3]\\
&\quad - \eta''\left[\int_\xi^1\int_0^\xi(\dot{\eta}'^2+\eta'\ddot{\eta}')\,\mathrm{d}\xi\mathrm{d}\xi + \int_\xi^1\left(\frac{1}{2}\dot{\mathscr{U}}\sqrt{\beta}\eta'^2 + 2\mathscr{U}\sqrt{\beta}\eta'\dot{\eta}' + \mathscr{U}^2\eta'\eta''\right)\mathrm{d}\xi\right]\\
&\quad + \eta'\int_0^\xi(\dot{\eta}'^2+\eta'\ddot{\eta}')\,\mathrm{d}\xi = 0,
\end{aligned} \tag{A.5}$$

where $\mathscr{U}$ is used instead of u for the dimensionless flow velocity, to avoid confusion for the pipe with supported ends.

For the pipe with supported ends, defining by u and v the displacements of the centreline along the undeformed axis and perpendicular to it, respectively, the equations of motion are

$$\begin{aligned}
&\ddot{\overline{u}} + 2\mathscr{U}\sqrt{\beta}\dot{\overline{u}}' + \mathscr{U}^2\overline{u}'' + \dot{\mathscr{U}}\sqrt{\beta}\overline{u}' - \mathscr{A}\overline{u}'' - (\overline{v}''\overline{v}''' + \overline{v}'\overline{v}'''')\\
&\quad + (\dot{\mathscr{U}}\sqrt{\beta}-\gamma)[\tfrac{1}{2}\overline{v}'^2 - (1-\xi)\overline{v}'\overline{v}''] + (\Gamma - \mathscr{A} - \Pi)\overline{v}'\overline{v}'' = 0,
\end{aligned} \tag{A.6}$$

$$\begin{aligned}
&\ddot{\overline{v}} + 2\mathscr{U}\sqrt{\beta}\dot{\overline{v}}' + \mathscr{U}^2\overline{v}'' - (\Gamma-\Pi)\overline{v}'' + \overline{v}'''' + \gamma\overline{v}' + (\Gamma - \mathscr{A} - \Pi)(\overline{u}''\overline{v}' + \overline{u}'\overline{v}'' + \tfrac{3}{2}\overline{v}'^2\overline{v}'')\\
&\quad - (3\overline{u}'''\overline{v}'' + 4\overline{u}''\overline{v}''' + 2\overline{u}'\overline{v}'''' + \overline{v}'\overline{u}'''' + 2\overline{v}''^3 + 2\overline{v}'^2\overline{v}'''' + 8\overline{v}'\overline{v}''\overline{v}''')\\
&\quad + (\dot{\mathscr{U}}\sqrt{\beta}-\gamma)[\overline{v}'\overline{u}' + \tfrac{1}{2}\overline{v}'^3 - (1-\xi)(-\overline{v}'' + \overline{u}''\overline{v}' + \overline{u}'\overline{v}'' + \tfrac{3}{2}\overline{v}'^2\overline{v}'')] = 0,
\end{aligned} \tag{A.7}$$

where $\overline{u} = u/L$, $\overline{v} = v/L$, the dimensionless tension $\Gamma = T(L)L^2/EI$, the axial flexibility $\mathscr{A} = EA\,L^2/EI$, and the pressure at the downstream end $\Pi = P(L)L^2/EI$.

The main purpose for providing the nonlinear equations in this appendix is to show how much more complicated they are, compared to Eq. (A.2), even though they are correct to only $\mathscr{O}(\varepsilon^3)$, where η and $\overline{v}$ are of $\mathscr{O}(\varepsilon)$.

Appendix B

B.1. Dynamics of aspirating pipes

Initially, it was thought that an aspirating pipe becomes unstable by flutter at infinitesimally small flow velocities if dissipative damping is neglected [90]. This conclusion was arrived at by replacing U by $-U$ in an equation similar to Eq. (1) but more appropriate to the ocean mining system. Then in Eq. (2), the signs are reversed, showing a positive energy transfer for small U. If dissipative forces are accounted for, the instability does not then occur at infinitesimally small U, but at very small U nonetheless.

This was later revised and related to Feynman's quandary on the direction of rotation of an aspirating rotary sprinkler [91], suggesting that flutter *never* arises. As pointed out by Kuiper and Metrikine [92], however, the "proof" was at best incomplete, and they suggested that the non-occurrence of flutter may be related to dissipative forces, in particular dissipation with the surrounding fluid (typically water).[6] This forced yet another re-evaluation of the stability of the system, by Païdoussis et al. [93], in which it was found that whether flutter occurs or not depends intimately on the details of the flow field in the vicinity of the intake.

Païdoussis et al. [93] presented two variants of the equation of motion and associated boundary conditions, differing as to the direction of the incoming flow. If this flow direction remains unchanged as the pipe

[6]Further work on this has recently been published [94].

oscillates, then flutter is shown to be impossible. If, however, as is more likely, the incoming flow is tangential to the pipe end, then flutter is possible; but whether it occurs or not depends on the flow field near the intake, currently being studied by CFD.

In this latter case, it is found that

$$\Delta W = -[1-(1-\alpha)(1+\overline{\gamma})]MU^2\int_0^T \left(\frac{\partial w}{\partial x}\frac{\partial w}{\partial t}\right)\Big|_L \mathrm{d}t,$$

where $\alpha = v/U$ is the ratio of the average flow velocity before entry into the pipe to that within the pipe, and $\overline{\gamma}$ is a tension effect on the pipe itself related to the flow near the intake. Typically $1-\alpha > 0.5$ and $1.7 < 1+\overline{\gamma} < 2.4$. Taking $1-\alpha = 0.6$ and $1+\overline{\gamma} = 2$, for example, one obtains $\Delta W = +0.2MU^2\int_0^T \left[(\partial w/\partial x)(\partial w/\partial t)\right]_L \mathrm{d}t$. By the arguments for a discharging pipe, this would mean a negative work input if $\overline{[(\partial w/\partial x)(\partial w/\partial t)]_L} < 0$, and hence a stable system. However, the perfidiousness of the system is unbounded: if in one mode $\overline{[(\partial w/\partial x)(\partial w/\partial t)]_L}$ is negative, it is positive in another; so, energy can be extracted from the fluid in any case, unless $(1-\alpha)(1+\overline{\gamma}) = 1$ exactly. Hence, it seems likely that, in principle, an instability is possible if the flow enters tangentially. Nevertheless, the small factor multiplying MU^2, on the one hand, and dissipative forces, on the other, mean that instability occurs at flow velocities beyond the range of practical interest for the ocean mining application [93]; this also explains its non-occurrence in the experiments with the pipe immersed in water [3].

Still, some problems refuse to be neatly laid to rest. New experiments by Kuiper et al. [95], reported at the Delft EUROMECH 484 where this very paper was presented, delivered a truly Delphic statement as to whether such systems are susceptible to flutter or not: something like "they flutter nay remain stable", with the ambiguity being where one puts the semicolon. In the event, the ambiguity relates to what time one observes the system: at first it does not, then it does flutter, and later it stops again, and so on!

Appendix C

C.1. The equations of motion of a cylinder in axial flow

Consider a cylinder of cross-sectional area A, diameter D, length L, mass per unit length m, flexural rigidity EI, Poisson ratio v and Kelvin–Voigt damping coefficient E^*, immersed in a vertical arrangement in axial flow, so that $x = 0$ is at the upper, upstream end, and $x = L$ at the downstream end (see Fig. 5). The mean fluid velocity is U and the fluid density ρ. It is supposed that the cylinder may be subjected to an externally applied tension $\overline{T}$ and a fluid pressurization $\overline{p}$. Assuming an inextensible centreline, the equation of motion, a fuller form than Eq. (5), for small lateral motion $y(x,t)$ is [4, Chapter 8]

$$\begin{aligned}&\left(E^*\frac{\partial}{\partial t}+E\right)I\frac{\partial^4 y}{\partial x^4}+\rho A\left(\frac{\partial}{\partial t}+U\frac{\partial}{\partial x}\right)^2 y-\left\{\delta[\overline{T}+(1-2v)(\overline{p}A)]\right.\\&\quad+\left[\frac{1}{2}\rho DU^2C_T+(m-\rho A)g\right]\left[\left(1-\frac{1}{2}\delta\right)L-x\right]+\left.\frac{1}{2}\rho D^2U^2(1-\delta)C_b\right\}\frac{\partial^2 y}{\partial x^2}\\&\quad+\frac{1}{2}\rho DUC_N\left(\frac{\partial y}{\partial t}+U\frac{\partial y}{\partial x}\right)+\frac{1}{2}\rho DC_D\frac{\partial y}{\partial t}+(m-\rho A)g\frac{\partial y}{\partial x}+m\frac{\partial^2 y}{\partial t^2}=0,\end{aligned}\tag{C.1}$$

where C_N, C_T, C_D and C_b have been defined in Section 3.1; $\delta = 0$ signifies that the downstream end is free to slide axially, and $\delta = 1$ if the supports do not allow net axial extension.

In this equation, ρA is the virtual or "added" mass of the fluid per unit length, which applies to unconfined flow. If the flow is confined, e.g. by being contained in an outer cylindrical conduit, then this added mass becomes $\chi\rho A$. For cylindrical confinement, $\chi = [(D_{ch}^2 + D^2)/(D_{ch}^2 - D^2)] > 1$ increases with increasing

confinement; $D_{ch} = 2R_0$ is the diameter of the flow-channel. In this case, the equation of motion becomes

$$\left(E^*\frac{\partial}{\partial t}+E\right)I\frac{\partial^4 y}{\partial x^4}+\chi\rho A\left(\frac{\partial}{\partial t}+U\frac{\partial}{\partial x}\right)^2 y-\left\{\delta[\overline{T}+(1-2v)(\overline{p}A)]\right.$$
$$+\left[\frac{1}{2}\rho DU^2C_f\left(1+\frac{D}{D_h}\right)+(m-\rho A)g\right]\left[\left(1-\frac{1}{2}\delta\right)L-x\right]$$
$$\left.+\frac{1}{2}\rho D^2U^2(1-\delta)C_b\right\}\frac{\partial^2 y}{\partial x^2}+\frac{1}{2}\rho DUC_f\left(\frac{\partial y}{\partial t}+U\frac{\partial y}{\partial x}\right)+\frac{1}{2}\rho DC_D\frac{\partial y}{\partial t}$$
$$+\left[(m-\rho A)g+\frac{1}{2}\rho DU^2C_f\left(\frac{D}{D_h}\right)\right]\frac{\partial y}{\partial x}+m\frac{\partial^2 y}{\partial t^2}=0, \tag{C.2}$$

where $D_h = 4A_{ch}/S_{tot}$ is the hydraulic diameter, and $C_N = C_T = C_f$ has been used for simplicity.

The boundary conditions have been discussed briefly in Section 3.1 and more fully in Ref. [4].

Defining the dimensionless quantities

$$\xi = x/L, \quad \eta = y/L \quad \text{and} \quad \tau = \{EI/(m+\rho A)\}^{1/2}t/L^2.$$

$$\alpha = \left[\frac{I}{E(\rho A+m)}\right]^{1/2}\frac{E^*}{L^2}, \quad \beta = \frac{\rho A}{\rho A+m}, \quad \gamma = \frac{(m-\rho A)g\,L^3}{EI}, \quad \Gamma = \frac{\overline{T}L^2}{EI},$$
$$\varepsilon = \frac{L}{D}, \quad u = \left(\frac{\rho A}{EI}\right)^{1/2}UL, \quad \Pi = \frac{\overline{p}A\,L^2}{EI}, \quad h = \frac{D}{D_h}, \quad c_f = \frac{4}{\pi}C_f,$$
$$c_N = \frac{4}{\pi}C_N, \quad c_T = \frac{4}{\pi}C_T, \quad c_b = \frac{4}{\pi}C_b, \quad c = \frac{4}{\pi}\left(\frac{\rho A}{EI}\right)^{1/2}LC_D, \tag{C.3}$$

the dimensionless forms of Eqs. (C.1) and (C.2) are

$$\left(\alpha\frac{\partial}{\partial\tau}+1\right)\frac{\partial^4\eta}{\partial\xi^4}+\left\{u^2-\delta[\Gamma+(1-2v)\Pi]-\left[\frac{1}{2}\varepsilon c_Tu^2+\gamma\right]\left[\left(1-\frac{1}{2}\delta\right)-\xi\right]\right.$$
$$\left.-\frac{1}{2}(1-\delta)c_bu^2\right\}\frac{\partial^2\eta}{\partial\xi^2}+2\beta^{1/2}u\frac{\partial^2\eta}{\partial\xi\partial\tau}+\left[\frac{1}{2}\varepsilon c_Nu^2+\gamma\right]\frac{\partial\eta}{\partial\xi}$$
$$+\left[\frac{1}{2}\varepsilon c_N\beta^{1/2}u+\frac{1}{2}\varepsilon c\beta^{1/2}\right]\frac{\partial\eta}{\partial\tau}+\frac{\partial^2\eta}{\partial\tau^2}=0 \tag{C.4}$$

and

$$\alpha\frac{\partial^5\eta}{\partial\xi^4\partial\tau}+\frac{\partial^4\eta}{\partial\xi^4}+\left\{\chi u^2-\delta[\Gamma+(1-2v)\Pi]-\left[\frac{1}{2}\varepsilon c_fu^2(1+h)+\gamma\right]\left[\left(1-\frac{1}{2}\delta\right)-\xi\right]\right.$$
$$\left.-\frac{1}{2}(1-\delta)c_bu^2\right\}\frac{\partial^2\eta}{\partial\xi^2}+2\chi\beta^{1/2}u\frac{\partial^2\eta}{\partial\xi\partial\tau}+\left[\frac{1}{2}\varepsilon c_fu^2(1+h)+\gamma\right]\frac{\partial\eta}{\partial\xi}$$
$$+\left[\frac{1}{2}\varepsilon c_f\beta^{1/2}u+\frac{1}{2}\varepsilon c\beta^{1/2}\right]\frac{\partial\eta}{\partial\tau}+[1+(\chi-1)\beta]\frac{\partial^2\eta}{\partial\tau^2}=0. \tag{C.5}$$

The dimensionless frequency ω is defined as

$$\omega = \left(\frac{\rho A+m}{EI}\right)^{1/2}\Omega\,L^2 \tag{C.6}$$

in terms of the radian frequency Ω.

If the centreline is extensible, then the system is governed by a pair of equations of motion—cf. the last two equations of Appendix A; refer to Refs. [4, Appendix T; 32].

Appendix D

D.1. The equations of motion of a cylindrical shell subjected to internal or external axial flow

Flügge's [96] equations of motion for a thin cylindrical shell, modified to take into account fluid loading associated with an internal pressure p_i and an external pressure p_o, are:

$$\begin{aligned}
\mathscr{L}_1(u,v,w) &= u'' + \frac{1-\nu}{2}\ddot{u} + \frac{1+\nu}{2}\dot{v}' + \nu w' + k\left[\frac{1-\nu}{2}\ddot{u} - w''' + \frac{1-\nu}{2}\ddot{w}'\right] = \gamma\frac{\partial^2 u}{\partial t^2},\\
\mathscr{L}_2(u,v,w) &= \frac{1+\nu}{2}u' + \ddot{v} + \frac{1-\nu}{2}v'' + \dot{w} + k\left[\frac{3}{2}(1-\nu)v'' - \frac{3-\nu}{2}\ddot{w}'\right] = \gamma\frac{\partial^2 v}{\partial t^2},\\
\mathscr{L}_3(u,v,w) &= \nu u' + \dot{v} + w + k\left[\frac{1-\nu}{2}\ddot{u}' - u''' - \frac{3-\nu}{2}\ddot{v}' + \nabla^4 w + 2\ddot{w} + w\right]\\
&= -\gamma\left[\frac{\partial^2 w}{\partial t^2} - \frac{q_r}{\rho_s h}\right],
\end{aligned} \tag{D.1}$$

where

$$k = \tfrac{1}{12}(h/a)^2, \quad \gamma = \rho_s a^2(1-\nu^2)/E,$$

$$(\ )' = a\partial(\ )/\partial x, \quad (\ )\dot{} = \partial(\ )/\partial\theta, \quad \nabla^2 = a^2(\partial^2/\partial x^2) + \partial^2/\partial\theta^2, \tag{D.2}$$

ρ_s being the density of the shell material and $q_r = (p_i - p_o)|_{r=a}$; the last equation has been multiplied by -1, to achieve symmetry of the operator-matrix of the left-hand side. The following two mass parameters are also important to fully define the system:

$$\mu_i = \frac{\rho_i a}{\rho_s h}, \quad \mu_e = \frac{\rho_e a}{\rho_s h}, \tag{D.3}$$

where ρ_i and ρ_e are the densities of the fluid in and out of the shell, respectively, h is the wall thickness and a the shell radius.

For a clamped end, the boundary conditions are

$$u = v = w = 0, \quad w' = 0. \tag{D.4}$$

For a free end they are

$$\begin{aligned}
u' + \nu\dot{v} + \nu w - kw'' &= 0,\\
w'' + \nu\ddot{w} - \nu\dot{v} - u' &= 0,\\
w''' + (2-\nu)\ddot{w}' - \frac{3-\nu}{2}\dot{v}' + \frac{1-\nu}{2}\ddot{u} - u'' &= 0,\\
\dot{u} + v' + 3k(v' - \dot{w}') &= 0.
\end{aligned} \tag{D.5}$$

If the steady viscous effects—associated with a varying pressure due to frictional pressure loss, for the case of internal flow, and surface traction—are taken into account, then, using the notation of Eq. (9), the equations of motion become

$$\begin{aligned}
\mathscr{L}_1(u,v,w) + q_1 u'' + q_2(\dot{v} + w) + q_3(\ddot{u} - w') &= \gamma(\partial^2 u/\partial t^2),\\
\mathscr{L}_2(u,v,w) + q_1 v'' + q_3(\ddot{v} + \dot{w}) &= \gamma(\partial^2 v/\partial t^2),\\
\mathscr{L}_3(u,v,w) - q_1 w'' - q_3(u' - \dot{v} + \ddot{w}) &= -\gamma[(\partial^2 w/\partial t^2) - q_r/\rho_s h],
\end{aligned} \tag{D.6}$$

where $\mathscr{L}_i(u,v,w)$, $i=1,2,3$, are as in Eqs. (9), $q_r=(p_i-p_o)|_{r=a}$ is the perturbation pressure associated with shell motions [4, Section 7.2.3], and

$$\{q_1,q_2,q_3\}=[(1-\nu^2)/Eh]\{\overline{N}_x,a\overline{p}_x,a\overline{p}_r\}, \tag{D.7}$$

in which

$$\overline{N}_x=B(\tfrac{1}{2}L-x)-\nu a(\tfrac{1}{2}LC+D),\quad \overline{N}_\theta=-a(Cx+D) \tag{D.8}$$

and

$$\overline{p}_x=B,\quad \overline{p}_r=-(Cx+D); \tag{D.9}$$

B, C, D are constants to be determined in each particular case. In this, it has been assumed that the form of the axial (traction) and radial (pressure-related) stresses is as in Eqs. (D.8).

Nonlinear computations have generally been done by means of the Donnell nonlinear shallow-shell equations. These are not given here for brevity, but may be found in Refs. [4,70,71,74], for instance.

References

[1] M.P. Païdoussis, G.X. Li, Pipes conveying fluid: a model dynamical problem, *Journal of Fluids and Structures* 7 (1993) 137–204.
[2] R.E.D. Bishop, I. Fawzy, Free and forced oscillation of a vertical tube containing a flowing fluid, *Philosophical Transactions, The Royal Society (London)* 284 (1976) 1–47.
[3] M.P. Païdoussis, *Fluid–Structure Interactions: Slender Structures and Axial Flow*, Vol. 1, Academic Press, London, 1998.
[4] M.P. Païdoussis, *Fluid–Structure Interactions: Slender Structures and Axial Flow*, Vol. 2, Elsevier Academic Press, London, 2004.
[5] T.B. Benjamin, Dynamics of a system of articulated pipes conveying fluid. I. Theory, *Proceedings of the Royal Society (London) A* 261 (1961) 457–486.
[6] R.W. Gregory, M.P. Païdoussis, Unstable oscillation of tubular cantilevers conveying fluid. I. Theory, *Proceedings of the Royal Society (London) A* 293 (1966) 512–527.
[7] T.B. Benjamin, Dynamics of a system of articulated pipes conveying fluid. II. Experiments, *Proceedings of the Royal Society (London) A* 261 (1961) 487–499.
[8] H. Ziegler, *Principles of Structural Stability*, Blaisdell, Waltham, MA, 1968.
[9] M.P. Païdoussis, Dynamics of tubular cantilevers conveying fluid, *Journal of Mechanical Engineering Science* 12 (1970) 85–103.
[10] F.-J. Bourrières, Sur un phénomène d'oscillation auto-entretenue en mécanique des fluides réels, *Publications Scientifiques et Techniques du Ministère de l'Air*, 1939, No. 147.
[11] R.W. Gregory, M.P. Païdoussis, Unstable oscillation of tubular cantilevers conveying fluid. II. Experiments, *Proceedings of the Royal Society (London) A* 293 (1966) 528–542.
[12] M.P. Païdoussis, N.T. Issid, Dynamic stability of pipes conveying fluid, *Journal of Sound and Vibration* 33 (1974) 267–294.
[13] A.N. Kounadis, Flutter instability and other singularity phenomena in symmetric systems via combination of mass distribution and weak damping, *International Journal of Non-Linear Mechanics* (2002), submitted for publication.
[14] G.T.S. Done, A. Simpson, Dynamic stability of certain conservative and non-conservative systems, *I. Mech. E. Journal of Mechanical Engineering Science* 19 (1977) 251–263.
[15] P.J. Holmes, Bifurcations to divergence and flutter in flow-induced oscillations: a finite-dimensional analysis, *Journal of Sound and Vibration* 53 (1977) 471–503.
[16] P.J. Holmes, Pipes supported at both ends cannot flutter, *Journal of Applied Mechanics* 45 (1978) 619–622.
[17] M. Yoshizawa, H. Nao, E. Hasegawa, Y. Tsujioka, Buckling and postbuckling behavior of a flexible pipe conveying fluid, *Bulletin of JSME* 28 (240) (1985) 1218–1225.
[18] Y. Modarres-Sadeghi, M.P. Païdoussis, A. Camargo, The behaviour of fluid-conveying pipes, supported at both ends, by the complete extensible nonlinear equations of motion, in: M.P. Païdoussis (Ed.), *Proceedings of the 6th FSI, AE & FIV+N Symposium*, Vancouver, Canada, ASME, New York, 2006, Proceedings of the ASME PVP Conference, 2006, Vol. 4, Part A, pp. 739–745.
[19] A.K. Bajaj, P.R. Sethna, T.S. Lundgren, Hopf bifurcation phenomena in tubes carrying fluid, *SIAM Journal of Applied Mathematics* 39 (1980) 213–230.
[20] A.K. Bajaj, P.R. Sethna, Effect of symmetry-breaking perturbations on flow-induced oscillations in tubes, *Journal of Fluids and Structures* 5 (1991) 651–679.
[21] J.M.T. Thompson, 'Paradoxial' mechanics under fluid flow, *Nature* 296 (1982) 135–137.
[22] A.S. Greenwald, J. Dugundji, Static and dynamic instabilities of a propellant line, AFOSR Science Report: AFOSR 67-1395, MIT Aeroelastic and Structures Research Lab, 1967.
[23] T.B. Benjamin, The threefold classification of disturbances in flexible surfaces bounding inviscid flows, *Journal of Fluid Mechanics* 16 (1963) 436–450.
[24] A. Steindl, H. Troger, Nonlinear three-dimensional oscillations of elastically constrained fluid conveying viscoelastic tubes with perfect broken $\mathscr{O}(2)$-symmetry, *Nonlinear Dynamics* 7 (1995) 165–193.

[25] G.S. Copeland, F.C. Moon, Chaotic flow-induced vibration of a flexible tube with end mass, *Journal of Fluids and Structures* 6 (1992) 705–718.
[26] M.P. Païdoussis, C. Semler, Non-linear dynamics of a fluid-conveying cantilevered pipe with a small mass attached at the free end, *Journal of Non-Linear Mechanics* 33 (1998) 15–32.
[27] M.P. Païdoussis, Hydroelastic ichthyoid propulsion, *AIAA Journal of Hydronautics* 10 (1976) 30–32.
[28] M.P. Païdoussis, The 1992 Calvin Rice Lecture: some curiosity-driven research in fluid–structure interactions and its current applications, *ASME Journal of Pressure Vessel Technology* 115 (1993) 2–14.
[29] M.P. Païdoussis, Dynamics of cylindrical structures subjected to axial flow, *Journal of Sound and Vibration* 29 (1973) 365–385.
[30] W.R. Hawthorne, The early development of the Dracone flexible barge, *Proceedings of the Institution of Mechanical Engineers* 175 (1961) 52–83.
[31] M.P. Païdoussis, Dynamics of flexible slender cylinders in axial flow. Part 2: experiments, *Journal of Fluid Mechanics* 26 (1966) 737–751.
[32] Y. Modarres-Sadeghi, M.P. Païdoussis, C. Semler, A nonlinear model for an extensible slender flexible cylinder subjected to axial flow, *Journal of Fluids and Structures* 21 (2005) 609–627 Addendum: 22 (2006) 597.
[33] Y. Modarres-Sadeghi, M.P. Païdoussis, C. Semler, E. Grinevich, Experiments on vertical slender flexible cylinders clamped at both ends and subjected to axial flow, *Philosophical Transactions of the Royal Society* (*London*) (2006), accepted for publication.
[34] M.S. Triantafyllou, Private communication, 3 November 1998.
[35] M.P. Païdoussis, E. Grinevich, D. Adamovic, C. Semler, Linear and nonlinear dynamics of cantilevered cylinders in axial flow. Part 1: physical dynamics, *Journal of Fluids and Structures* 16 (2002) 691–713.
[36] J.-L. Lopes, M.P. Païdoussis, C. Semler, Linear and nonlinear dynamics of cantilevered cylinders in axial flow. Part 2: the equations of motion, *Journal of Fluids and Structures* 16 (2002) 715–737.
[37] C. Semler, J.-L. Lopes, N. Augu, M.P. Païdoussis, Linear and nonlinear dynamics of cantilevered cylinders in axial flow. Part 3: nonlinear dynamics, *Journal of Fluids and Structures* 16 (2002) 739–759.
[38] A.P. Dowling, The dynamics of towed flexible cylinders. Part 1: neutrally buoyant elements, *Journal of Fluid Mechanics* 187 (1988) 507–532.
[39] C.C. Ni, R.J. Hansen, An experimental study of the flow-induced motions of a flexible cylinder in axial flow, *ASME Journal of Fluids Engineering* 100 (1978) 389–394 Discussion 101 (1979) 292–293; 102 (1980) 119.
[40] C. Lemaitre, P. Hémon, E. de Langre, Instability of a long ribbon hanging in axial air flow, *Journal of Fluids and Structures* 21 (2005) 913–925.
[41] E. de Langre, M.P. Païdoussis, O. Doaré, Y. Modarres-Sadeghi, Flutter of long flexible cylinders in axial flow, *Journal of Fluid Mechanics* 571 (2007) 371–389.
[42] S.S. Chen, *Flow-Induced Vibration of Circular Structures*, Hemisphere, Washington, 1987.
[43] M.P. Païdoussis, The dynamics of clusters of flexible cylinders in axial flow: theory and experiments, *Journal of Sound and Vibration* 65 (1979) 391–417.
[44] M.P. Païdoussis, The amplitude of fluid-induced vibration of cylinders in axial flow, Atomic Energy of Canada Report AECL-2225, 1965.
[45] M.P. Païdoussis, An experimental study of vibration of flexible cylinders induced by nominally axial flow, *Nuclear Science and Engineering* 35 (1969) 127–138.
[46] M.P. Païdoussis, Vibrations of cylindrical structures subjected to axial flow, *ASME Journal of Engineering for Industry* 96 (1974) 547–552.
[47] M.P. Païdoussis, Flow-induced vibrations in nuclear reactors and heat exchangers: practical experiences and state of the knowledge, in: E. Naudascher, D. Rockwell (Eds.), *Practical Experiences with Flow-Induced Vibrations*, Springer, Berlin, 1980, pp. 1–81.
[48] I.A. Taleb, A.K. Misra, Dynamics of an axially moving beam submerged in a fluid, *AIAA Journal of Hydronautics* 15 (1981) 62–66.
[49] F. Gosselin, M.P. Païdoussis, A.K. Misra, Stability of a deploying/extruding beam in dense fluid, *Journal of Sound and Vibration* 299 (2007) 123–142.
[50] M.P. Païdoussis, Ll.R. Curling, An analytical model for vibration of clusters of flexible cylinders in turbulent axial flow, *Journal of Sound and Vibration* 98 (1985) 493–517.
[51] Ll. Curling, M.P. Païdoussis, Analyses for random flow-induced vibration of cylindrical structures subjected to turbulent axial flow, *Journal of Sound and Vibration* 264 (2003) 795–833.
[52] J.O. Gagnon, M.P. Païdoussis, Fluid coupling characteristics and vibration of cylinder clusters in axial flow. Part I: theory, *Journal of Fluids and Structures* 8 (1994) 257–291.
[53] J.O. Gagnon, M.P. Païdoussis, Fluid coupling characteristics and vibration of cylinder clusters in axial flow. Part II: experiments, *Journal of Fluids and Structures* 8 (1994) 293–324.
[54] M.P. Païdoussis, Stability of towed, totally submerged flexible cylinders, *Journal of Fluid Mechanics* 34 (1968) 273–297.
[55] V.I. Poddubny, J.E. Shamarin, D.A. Chernko, L.S. Astakhov, *Dynamics of Undersea Towing Systems*, Sudostroenye, St. Petersburg, 1995.
[56] K. Sudarsan, S.K. Bhattacharyya, C.P. Vendhan, An experimental study of hydroelastic instability of flexible towed underwater cylindrical structures, *Proceedings 16th OMAE Conference*, Vol. A, Yokohama, Japan, ASME, New York, 1997, pp. 73–80.
[57] H. Sarv, J. John, Technical and economical aspects of large-scale CO_2 storage in deep oceans, *Proceedings 25th International Technical Conference on Coal Utilization and Fuel Systems*, Vol. 1, Paper MTI-00-03, 2000, Clearwater, FL, USA.
[58] N. Hamy, *The Trebron Sea Chain System*, Trebron Holdings Ltd., Montreal, Québec, Canada, 1971.

[59] V.I. Poddubny, N.V. Saltanov, Three-dimensional parametric vibrations of filaments or wires in coaxial flows, *Fluid Mechanics Soviet Research* 20 (1991) 33–41.
[60] T.C. Papanastasiou, G.C. Georgiou, A.N. Alexandrou, *Viscous Fluid Flow*, CRC Press, Boca Raton, 2000.
[61] S. Kaneko, Y. Ozaki, T. Watanabe, Optical fiber cable vibrations induced by leakage-flow during coating process, in: M.P. Païdoussis et al. (Eds.), *Proceedings 5th International Symposium on FSI, AE & FIV+N*, New Orleans, LA, USA, ASME, New York, 2002.
[62] M. Hamadiche, H. Abou-Shady, Optical fiber instability during coating process, *Journal of Fluids and Structures* 22 (2006) 599–615.
[63] Y. Sakuma, M.P. Païdoussis, S.J. Price, Dynamics of trains and train-like articulated systems travelling in confined fluid. Parts 1 and 2, *Journal of Fluids and Structures*, submitted for publication.
[64] Y. Sakuma, Dynamics of Trains and Train-like Articulated Systems Travelling in Confined Fluid, PhD Thesis, McGill University, 2005.
[65] M.P. Païdoussis, J.-P. Denise, Flutter of thin cylindrical shells conveying fluid, *Journal of Sound and Vibration* 20 (1972) 9–26.
[66] A.W. Leissa, *Vibration of Shells*. NASA Report SP-288, 1973. Reprinted in book form by the Acoustical Society of America in 1993.
[67] V.B. Nguyen, M.P. Païdoussis, A.K. Misra, An experimental study of the stability of cantilevered coaxial cylindrical shells conveying fluid, *Journal of Fluids and Structures* 7 (1993) 913–930.
[68] A. El Chebair, M.P. Païdoussis, A.K. Misra, Experimental study of annular flow-induced instabilities of cylindrical shells, *Journal of Fluids and Structures* 3 (1989) 349–364.
[69] K.N. Karagiozis, M.P. Païdoussis, A.K. Misra, E. Grinevich, An experimental study of the nonlinear dynamics of cylindrical shells with clamped ends subjected to axial flow, *Journal of Fluids and Structures* 20 (2005) 801–816.
[70] K.N. Karagiozis, M.P. Païdoussis, M. Amabili, A.K. Misra, Nonlinear stability of cylindrical shells subjected to axial flow: theory and experiments, *Journal of Sound and Vibration* (2006), accepted for publication.
[71] K.N. Karagiozis, M.P. Païdoussis, A.K. Misra, Transmural pressure effects on the stability of clamped cylindrical shells subjected to internal fluid flow, *International Journal of Non-Linear Mechanics* (2006), accepted for publication.
[72] M.P. Païdoussis, Some unresolved issues in fluid–structure interactions, *Journal of Fluids and Structures* 20 (2005) 871–890.
[73] K.N. Karagiozis, M.P. Païdoussis, E. Grinevich, A.K. Misra, M. Amabili, Stability and nonlinear dynamics of clamped circular cylindrical shells in contact with flowing fluid, *Proceedings IUTAM Symposium on Integrated Modeling of Fully Coupled Fluid Structure Interactions*, Kluwer, Dordrecht, 2003, pp. 375–390.
[74] M. Amabili, F. Pellicano, M.P. Païdoussis, Nonlinear dynamics and stability of circular cylindrical shells containing flowing fluid. I. Stability, *Journal of Sound and Vibration* 225 (1999) 655–699.
[75] E.H. Dowell, *Aeroelasticity of Plates and Shells*, Noordhoff International Publishing, Leyden, 1975.
[76] E.F. Crawley, H.C. Curtiss, Jr., D.A. Peters, R.H. Scanlan, F. Sisto, in: E.H. Dowell (Ed.), *A Modern Course in Aeroelasticity*, third ed., Kluwer Academic Publishers, Dordrecht, 1995.
[77] C.D. Bertram, The dynamics of collapsible tubes, in: C.P. Ellington, T.J. Pedley (Eds.), *Biological Fluid Dynamics*, 1995, pp. 253–264.
[78] C.P. Ellington, T.J. Pedley, *Biological Fluid Dynamics*, Society for Experimental Biology, Cambridge, 1995.
[79] A. Kornecki, E.H. Dowell, J. O'Brien, On the aeroelastic instability of two-dimensional panels in uniform incompressible flow, *Journal of Sound and Vibration* 47 (1976) 163–178.
[80] C.Q. Guo, M.P. Païdoussis, Stability of rectangular plates with free-edges in two-dimensional inviscid channel flow, *Journal of Applied Mechanics* 67 (2000) 171–176.
[81] J. Dugundji, E.H. Dowell, B. Perkins, Subsonic flutter of panels on continuous elastic foundations, *AIAA Journal* 1 (1963) 1146–1154.
[82] T. Ishii, Aeroelastic instabilities of simply supported panels in subsonic flow, AIAA paper 65-772, 1965.
[83] D.S. Weaver, T.E. Unny, Hydroelastic stability of a flat plate, *Journal of Applied Mechanics* 37 (1970) 823–827.
[84] C.H. Ellen, The stability of simply supported rectangular surfaces in uniform subsonic flow, *Journal of Applied Mechanics* 40 (1973) 68–72.
[85] Y. Watanabe, S. Suzuki, M. Sugihara, Y. Sueoka, An experimental study of paper flutter, *Journal of Fluids and Structures* 16 (2002) 529–542.
[86] L. Tang, M.P. Païdoussis, On the instability and the post-critical behaviour of two-dimensional cantilevered flexible plates in axial flow, *Journal of Sound and Vibration* (2006), in press, doi:10.1016/j.jsv.2007.03.042.
[87] L. Tang, M.P. Païdoussis, The influence of the wake on the stability of cantilevered flexible plates in axial flow, *Journal of Sound and Vibration* (2006), accepted for publication.
[88] M.P. Païdoussis, Real-life experiences with flow-induced vibration, *Journal of Fluids and Structures* 22 (2006) 741–755.
[89] M.P. Païdoussis, D.T.-M. Wong, Flutter of thin cylindrical shells in cross flow, *Journal of Fluid Mechanics* 115 (1982) 411–426.
[90] M.P. Païdoussis, T.P. Luu, Dynamics of a pipe aspirating fluid, such as might be used in ocean mining, *ASME Journal of Energy Resources Technology* 107 (1985) 250–255.
[91] M.P. Païdoussis, Aspirating pipes do not flutter at infinitesimally small flow, *Journal of Fluids and Structures* 13 (1999) 419–425.
[92] G.L. Kuiper, A.V. Metrikine, Stability of submerged aspirating pipe: the effect of fluid depressurization at the inlet, *Journal of Sound and Vibration* 280 (2005) 1051–1065.
[93] M.P. Païdoussis, C. Semler, M. Wadham-Gagnon, A reappraisal of why aspirating pipes do not flutter at infinitesimal flow, *Journal of Fluids and Structures* 20 (2005) 147–156.
[94] G.L. Kuiper, A.V. Metrikine, J.A. Battjes, A new time-domain description and its influence on the dynamic behaviour of a cantilever pipe conveying fluid, *Journal of Fluids and Structures* 23 (2007) 429–445.
[95] G.L. Kuiper, A.V. Metrikine, Experimental investigation of dynamic stability of a free hanging pipe conveying fluid, *Book of Abstracts*, *EUROMECH* 484, 2006, pp. 37–38.
[96] W. Flügge, *W. Stresses in Shells*, Springer, Berlin, 1960.